Metal-Based Linear Light Upconversion Implemented in Molecular Complexes: Challenges and Perspectives

Hélène Bolvin, Alexandre Fürstenberg, Bahman Golesorkhi, Homayoun Nozary, Inès Taarit, Claude Piguet

ACCOUNTS of chemical research

pubs.acs.org/accounts

Article

Metal-Based Linear Light Upconversion Implemented in Molecular Complexes: Challenges and Perspectives

Hélène Bolvin, Alexandre Fürstenberg, Bahman Golesorkhi, Homayoun Nozary, Inès Taarit, and Claude Piguet*

Cite This: *Acc. Chem. Res.* 2022, 55, 442−456

Read Online

ACCESS | Metrics & More | Article Recommendations

CONSPECTUS: The piling up of low-energy photons to produce light beams of higher energies while exploiting the nonlinear optical response of matter was conceived theoretically around 1930 and demonstrated 30 years later with the help of the first coherent ruby lasers. The vanishingly small efficacy of the associated light-upconversion process was rapidly overcome by the implementation of powerful successive absorptions of two photons using linear optics in materials that possess real intermediate excited states working as relays. In these systems, the key point requires a favorable competition between the rate constant of the excited-state absorption (ESA) and the relaxation rate of the intermediate excited state, the lifetime of which should be thus maximized. Chemists and physicists therefore selected long-lived intermediate excited states found (i) in trivalent lanthanide cations doped into ionic solids or into nanoparticles ($^{2S+1}L_J$ spectroscopic levels) or (ii) in polyaromatic molecules (triplet states) as the logical activators for designing light upconverters using linear optics. Their global efficiency has been stepwise optimized during the past five decades by using indirect intermolecular sensitization mechanisms (energy transfer upconversion = ETU) combined with large absorption cross sections.

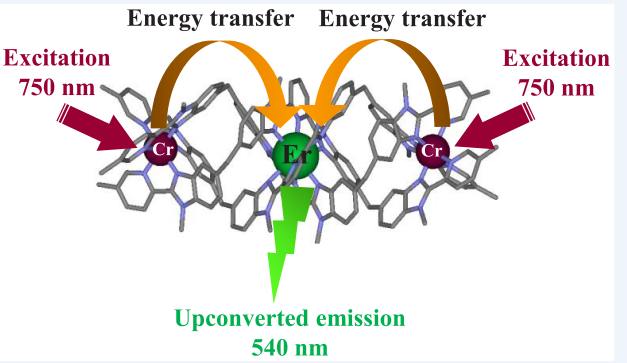

The induction of light-upconversion operating in a single discrete entity at the molecular level is limited to metal-based units and remained a challenge for a long time because coordination complexes possess high-frequency oscillators incompatible with the existence of (i) scales of accessible excited relays with long lifetimes and (ii) final high-energy emissive levels with noticeable intrinsic quantum yields. In contrast to intermolecular energy transfer processes operating in metal-based doped solids, which require statistical models, the combination of sensitizers and activators within the same molecule limits energy transfers to easily tunable intramolecular processes with first-order kinetic rate constants. Their successful programming in a trinuclear CrErCr complex in 2011 led to the first detectable near-infrared to green light upconversion induced in a molecular unit under reasonable excitation intensity. The subsequent progress in the modeling and understanding of the key factors controlling metal-based light upconversion operating in molecular complexes led to a burst of various designs exploiting different mechanisms, excited-state absorption (ESA), energy transfer upconversion (ETU), cooperative luminescence (CL), and cooperative upconversion (CU), which are discussed in this Account.

KEY REFERENCES

- Suffren, Y.; Zare, D.; Eliseeva, S. V.; Guénée, L.; Nozary, H.; Lathion, T.; Aboshyan-Sorgho, L.; Petoud, S.; Hauser, A.; Piguet, C. Near-Infrared to Visible Light-Upconversion in Molecules: From Dream to Reality. *J. Phys. Chem. C* **2013**, *117*, 26957−26963.[1] The original contribution that correlates the linear molecular-based upconversion process reported in 2011 with the energy transfer upconversion mechanism.
- Suffren, Y.; Golesorkhi, B.; Zare, D.; Guénée, L.; Nozary, H.; Eliseeva, S. V.; Petoud, S.; Hauser, A.; Piguet, C. Taming Lanthanide-Centered Upconversion at the Molecular Level. *Inorg. Chem.* **2016**, *55*, 9964−9972.[2] The first article addressing and reviewing the downscale processes that make light-upconversion compatible with molecular coordination complexes.
- Golesorkhi, B.; Taarit, I.; Bolvin, H.; Nozary, H.; Jimenez, J. R.; Besnard, C.; Guenee, L.; Furstenberg, A.; Piguet, C. Molecular Light-Upconversion: We Have Had a Prob-

Received: November 4, 2021
Published: January 24, 2022

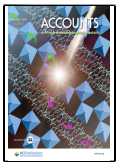

lem! When Excited State Absorption (ESA) Overcomes Energy Transfer Upconversion (ETU) in Cr(III)/Er(III) Complexes. *Dalton Trans.* **2021**, *50*, 7955−7968.[3] Discovery of the unexpectedly large erbium-based excited-state absorption processes, which reconcile single-center (ESA) and multicenter (ETU) light-upconversion efficiencies with the kinetic mechanisms operating at the molecular level.

- Golesorkhi, B.; Naseri, S.; Guénée, L.; Taarit, I.; Alves, F.; Nozary, H.; Piguet, C. Ligand-Sensitized Near-Infrared to Visible Linear Light Upconversion in a Discrete Molecular Erbium Complex. *J. Am. Chem. Soc.* **2021**, *143*, 15326−15334.[4] A gain in brightness by 6 orders of magnitude induced by improved absorption cross sections, which pushes molecular upconversion as an acceptable new topic for publication in high impact journals.

1. INTRODUCTION TO LIGHT UPCONVERSION

According to the law of degradation of energy, it seems rather obvious that excitation of a molecule using high-energy photons

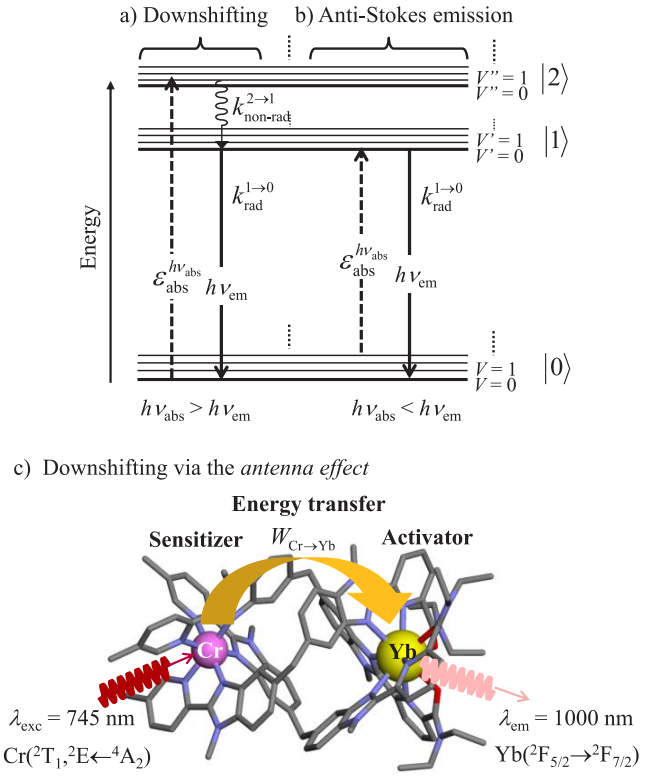

Figure 1. Three-level energy diagram with vibrational levels (V, V', and V'') showing linear optical processes: (a) light downshifting mechanism (excitation processes, dashed upward arrows; nonradiative multiphonon relaxation, undulating arrows; radiative emission processes, straight downward arrows); (b) anti-Stokes mechanism; (c) chemical illustration of light downshifting process exploiting the *antenna effect* operating in a molecular complex (data from ref 9).

($E = h\nu = hc/\lambda$ where ν is the frequency, λ is the wavelength, h is Planck's constant, and c is the speed of light in vacuum) may result in the emission of photons of lower frequency together with some complementary loss of energy in the form of heat due to nonradiative relaxation processes ($h\nu_{\text{abs}} > h\nu_{\text{em}}$, Figure 1a). The latter global process, referred to as linear light-downshifting,

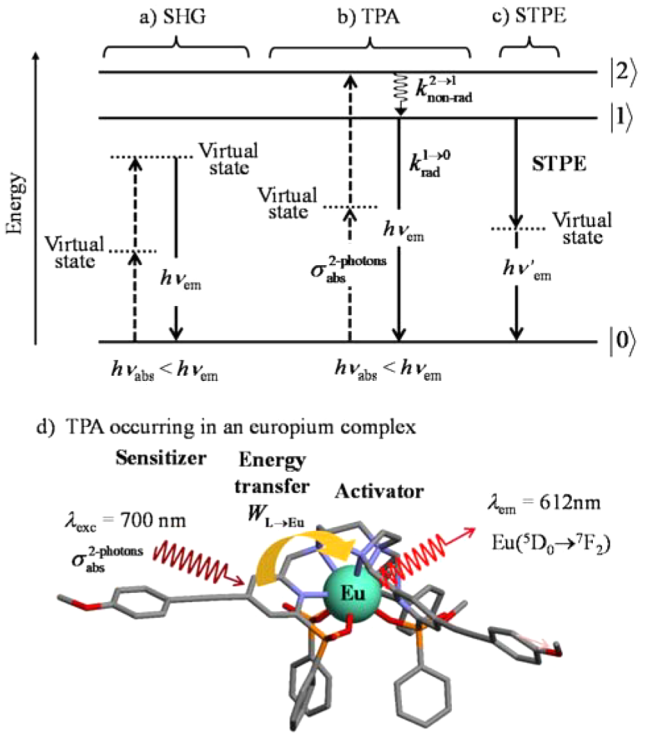

Figure 2. Three-level energy diagram showing nonlinear optical processes: (a) second-harmonic generation (SHG); (b) two-photon absorption (TPA); (c) spontaneous two-photon emission (STPE). (d) Chemical illustration of a NLO two-photon absorption operating in a molecular complex (data from ref 14).

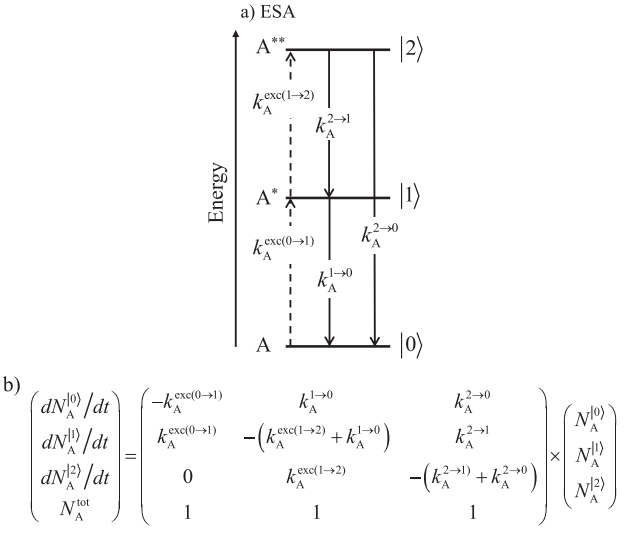

Figure 3. (a) Kinetic diagrams pertinent to linear upconversion operating under nonresonant excitation according to the single-center excited-state absorption (ESA) mechanism and (b) associated kinetic differential equations combined with the mass balance equation.

has a maximum quantum yield $\phi = 100\%$.[5] It has been observed in myriad organic molecules (p-block activators) or coordination complexes (d-block and f-block activators) where the ground state $|0\rangle$ and the absorbing $|2\rangle$ and emissive $|1\rangle$ levels are located either on the same optical center (Figure 1a) or on two different parts in the same molecule, which are tailored to exhibit (i) optimized light absorption for the sensitizer (S), (ii) maximum radiative emission for the activator (A), and (iii)

https://doi.org/10.1021/acs.accounts.1c00685
Acc. Chem. Res. 2022, 55, 442−456

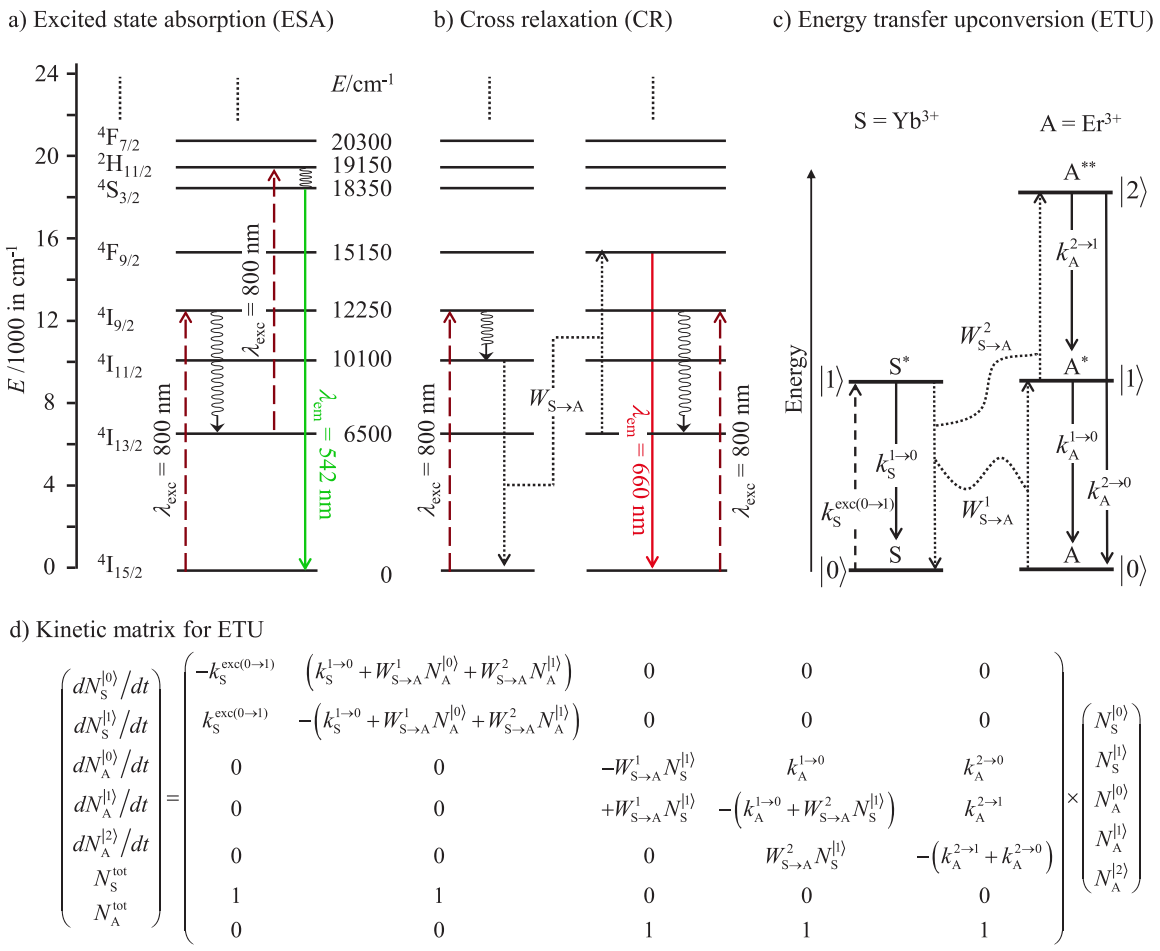

$$\begin{pmatrix} dN_S^{|0\rangle}/dt \\ dN_S^{|1\rangle}/dt \\ dN_A^{|0\rangle}/dt \\ dN_A^{|1\rangle}/dt \\ dN_A^{|2\rangle}/dt \\ N_S^{tot} \\ N_A^{tot} \end{pmatrix} = \begin{pmatrix} -k_S^{exc(0\to1)} & \left(k_S^{1\to0} + W_{S\to A}^1 N_A^{|0\rangle} + W_{S\to A}^2 N_A^{|1\rangle}\right) & 0 & 0 & 0 \\ k_S^{exc(0\to1)} & -\left(k_S^{1\to0} + W_{S\to A}^1 N_A^{|0\rangle} + W_{S\to A}^2 N_A^{|1\rangle}\right) & 0 & 0 & 0 \\ 0 & 0 & -W_{S\to A}^1 N_S^{|1\rangle} & k_A^{1\to0} & k_A^{2\to0} \\ 0 & 0 & +W_{S\to A}^1 N_S^{|1\rangle} & -\left(k_A^{1\to0} + W_{S\to A}^2 N_S^{|1\rangle}\right) & k_A^{2\to1} \\ 0 & 0 & 0 & W_{S\to A}^2 N_S^{|1\rangle} & -\left(k_A^{2\to1} + k_A^{2\to0}\right) \\ 1 & 1 & 0 & 0 & 0 \\ 0 & 0 & 1 & 1 & 1 \end{pmatrix} \times \begin{pmatrix} N_S^{|0\rangle} \\ N_S^{|1\rangle} \\ N_A^{|0\rangle} \\ N_A^{|1\rangle} \\ N_A^{|2\rangle} \end{pmatrix}$$

Figure 4. (a) Single-center excited-state absorption (ESA) and (b) multicenter cross relaxation (CR) upconversion mechanisms operating in Er^{3+}-doped $NaYF_4$-glass ceramics responsible for green and red upconverted emission observed upon near-infrared excitation at 800 nm. (c) Kinetic diagrams pertinent to linear upconversion operating under nonresonant excitation according to the multicenter energy transfer upconversion (ETU) mechanism for sensitizer/activator pairs in doped ionic solids and (d) associated kinetic differential equations combined with mass balance equations.

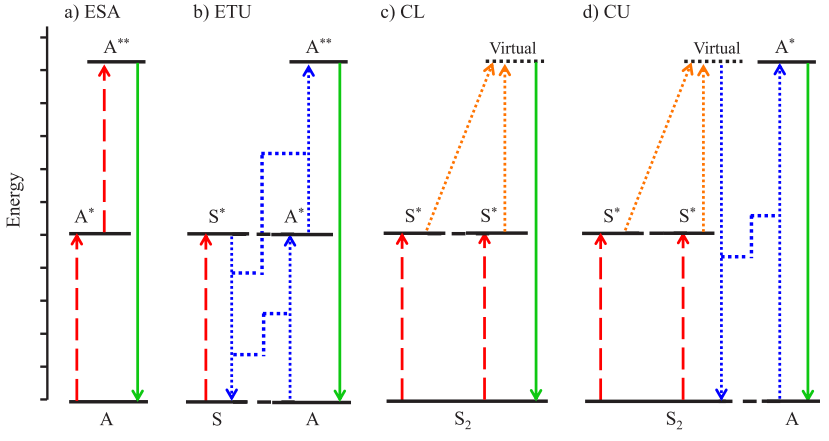

Figure 5. Schematic linear upconversion mechanisms operating in isolated molecules: (a) excited-state absorption (ESA), (b) energy transfer upconversion (ETU), (c) cooperative luminescence (CL), and)d) cooperative upconversion (CU). S, sensitizer, A, activator; red, linear excitation; blue, energy transfers; orange, two-center optical transitions; green, upconverted emission.

efficient S → A energy transfer leading to light-downshifting according to a mechanism called the *antenna effect* (Figure 1c).[6] The loss in energy between the absorbed and emitted photons is reminiscent of the Stokes shift and, since the latter energy gap is mainly transformed into heat, the temperature of the sample increases upon light irradiation. An alternative radiative decay route can be implemented when the molecule is excited into the long wavelength tail of its absorption spectrum so that the resulting luminescence is anti-Stokes shifted; in other words, the energy of the emitted photon is larger than that of the absorbed photon by a few kT (k is the Boltzmann constant and T is the temperature), which corresponds to the energy gap between the

https://doi.org/10.1021/acs.accounts.1c00685
Acc. Chem. Res. 2022, 55, 442−456

incriminated vibrational levels (hot bands, $h\nu_{abs} < h\nu_{em}$, Figure 1b).[7] Since the energy must be conserved, a molecule in an adiabatic system that decays by a radiative path to produce luminescence at higher energy is accompanied by a decrease in temperature of the sample. All anti-Stokes emissions that were known to exist before the 1960s involved emission energies in excess of excitation energies by only a few kT following mechanisms similar to that described in Figure 1b.[8]

However, the ability to combine two photons of low energy to produce an emitted photon of much higher energy (reminiscent of an anti-Stokes shift but larger than $(10-100)kT$) was predicted by Goeppert-Mayer in her thesis dedicated to the nonlinear optical (NLO) response of matter upon intense light irradiation in 1931 (Figure 2a).[10] It is worth remembering here that absorption of an electromagnetic wave by a molecule results from the polarization of the electron density by the alternating electric field (E) of the incident light beam. The polarization response $\Delta\mu = \alpha E + \beta E^2 + \gamma E^3 + ...$ involves electric polarizability (α of rank 1) together with first-order (β of rank 2) and second-order (γ of rank 3) hyperpolarizability tensors. α belongs to the realm of *linear optics*: its real part is involved in the calculation of the refractive index of the medium, whereas its imaginary part determines the one-photon absorption responsible for the excitation of a molecule from its ground state to its excited state (Figure 1). β quantifies all second-order *nonlinear optical* effects such as nonresonant second-harmonic generation (SHG, Figure 2a), while the imaginary part of the third-order γ tensor is responsible for *nonlinear* two-photon absorption (TPA, Figure 2b) with no need for the existence of real intermediate excited relays. Due to the faint NLO absorption coefficients β and γ, the experimental demonstration of the latter anti-Stokes processes was delayed until the early 1960s when intense coherent laser excitation beams became available.[10] Nowadays, access to ultraintense excitation beams with pulsed femtosecond lasers makes this field less esoteric with applications as probes in biology and as optical power limiting devices.[11] Obviously, the gain in energy is obtained at the cost of a maximum quantum yield of 50% (Figure 2b).

Interestingly, NLO is also compatible with spontaneous two-photon emission (STPE, Figure 2c),[12] which produces two photons of lower energies (quantum cutting or down-conversion) and a maximum quantum yield of 200% when excitation occurs through one-photon linear optics.[5] These NLO absorption (TPA) and emission (STPE) processes are at least 5−8 orders of magnitude less efficient than related one-photon linear processes,[8] so their exploitation in coordination chemistry dealing with (supra)molecular metallic complexes as activators remains scarce (Figure 2d).[13]

A breakthrough occurred in 1959 when Bloembergen proposed to excite the same optical center with two successive linear one-photon absorptions in order to develop an infrared quantum counter using a photomultiplier with visible spectrum sensitivity.[15] Soon after, Porter applied this idea for combining one infrared (IR) photon (λ_{exc} = 2300 nm, ν_{exc} = 4350 cm^{-1}) with one visible photon (λ_{exc} = 558 nm, ν_{exc} = 17920 cm^{-1}) upon continuous double excitation of crystals of $LaCl_3$ doped with Pr^{3+} activators.[16] Although the final emitted red photon at λ_{em} = 618 nm (ν_{em} = 16180 cm^{-1}) corresponds to an upconverted signal with respect to the IR excitation source only, the concept of using an intermediate excited state as a relay for the successive piling of two photons of lower energies via linear optical response to reach an emissive level of higher energy entered the physical community (Figure 3a).[8] The normalized population densities in each state $N_A^{|i\rangle}$ (i = 0, 1, or 2) obtained upon nonresonant excitation of a single-center activator obey the set of first-order differential equations summarized in the compact matrix formulation shown in Figure 3b, where $k_A^{i\to j}$ is the total relaxation rate constant (sum of radiative and nonradiative contributions) from level i to level j and $k_A^{exc(m\to n)}$ is the opposite pumping rate constant given in s^{-1} in eq 1. λ_P is the pump wavelength (in cm), P is the incident pump intensity (in W/cm^2), $\sigma_A^{m\to n}$ is the absorption cross section (in cm^2) of the activator-centered $m \to n$ transition related to the decadic molar absorption coefficient $\varepsilon^{m\to n}$ (in M^{-1}·cm^{-1}) according to $\sigma^{m\to n} = (3.8 \times 10^{-21})\varepsilon^{m\to n}$.[17]

$$k_A^{exc(m\to n)} = \frac{\lambda_P}{hc} P\sigma_A^{m\to n} = (3.8 \times 10^{-21})\frac{\lambda_P}{hc} P\varepsilon_A^{m\to n} \quad (1)$$

Upon continuous irradiation, the consecutive absorption of two photons according to the one-center excited-state absorption mechanism (ESA, Figure 3a) leads to steady-state population densities, $N_{A,s\text{-}s}^{|i\rangle}$, given in eqs 2 and 3, which are obtained by solving the set of first-order differential equations for $dN_A^{|i\rangle}/dt = 0$ (Figure 3b).[18]

$$N_{A,s\text{-}s}^{|1\rangle}(\mathrm{ESA}) = \frac{k_A^{exc(0\to 1)}(k_A^{2\to 1} + k_A^{2\to 0})}{k_A^{1\to 0}(k_A^{2\to 1} + k_A^{2\to 0}) + k_A^{2\to 0}k_A^{exc(1\to 2)}} N_{A,s\text{-}s}^{|0\rangle} \approx \left[\left(\frac{\lambda_P}{hc}\right)\sigma_A^{0\to 1} P\right]\tau_{A,obs}^{|1\rangle} N_A^{tot} \quad (2)$$

$$N_{A,s\text{-}s}^{|2\rangle}(\mathrm{ESA}) = \frac{k_A^{exc(0\to 1)}k_A^{exc(1\to 2)}}{k_A^{1\to 0}(k_A^{2\to 1} + k_A^{2\to 0}) + k_A^{2\to 0}k_A^{exc(1\to 2)}} N_{A,s\text{-}s}^{|0\rangle} \approx \left[\left(\frac{\lambda_P}{hc}\right)^2 \sigma_A^{0\to 1}\sigma_A^{1\to 2} P^2\right]\tau_{A,obs}^{|1\rangle}\tau_{A,obs}^{|2\rangle} N_A^{tot} \quad (3)$$

The dispersive terms $k_A^{2\to 0}k_A^{exc(1\to 2)}$ found in the denominators of eqs 2 and 3 are only important under massive excitation intensities that saturate the second excitation process. It is responsible for the deviation from the expected square dependence of the population of the upconverted level $N_{A,s\text{-}s}^{|2\rangle}$ on the incident pump intensity, P (eq 3). Under a reasonable continuous illumination regime, the latter term can be neglected and the major fraction of the activator remains in the ground state ($N_{A,s\text{-}s}^{|0\rangle} \simeq N_A^{tot}$) so that eqs 2 and 3 can be simplified to show that the upconverted population density $N_{A,s\text{-}s}^{|2\rangle}$ is proportional to (i) the square of the incident intensity (P^2), (ii) the product of the two successive absorption cross sections ($\sigma_A^{0\to 1}\sigma_A^{1\to 2}$), and (iii) the observed lifetimes ($\tau_{A,obs}^{|1\rangle}\tau_{A,obs}^{|2\rangle}$) of both excited states where $\tau_{A,obs}^{|1\rangle} = (k_A^{1\to 0})^{-1}$ and $\tau_{A,obs}^{|2\rangle} = (k_A^{2\to 1} + k_A^{2\to 0})^{-1}$ (eq 3, right part). Since the upconversion quantum yield of the ESA mechanism, $\phi_A^{up}(\mathrm{ESA})$, is itself proportional to $N_{A,s\text{-}s}^{|2\rangle}$ (eq 4), it was early recognized that systems possessing a scale of regularly spaced excited states with long lifetimes would be the best candidates for implementing efficient successive photon absorption ($\eta_A^{up}(\mathrm{ESA})$) prior to reaching a high-energy emissive level with a large intrinsic quantum yield $\phi_A = k_{A,rad}^{2\to 0}\tau_{A,obs}^{|2\rangle}$.

https://doi.org/10.1021/acs.accounts.1c00685
Acc. Chem. Res. 2022, 55, 442−456

$$\phi_A^{up}(\mathrm{ESA}) = \frac{\text{emitted photons}}{\text{absorbed photons}} = \frac{k_{A,rad}^{2\to0} N_{A,s\text{-}s}^{|2\rangle}}{k_A^{exc(0\to1)} N_{A,s\text{-}s}^{|0\rangle} + k_A^{exc(1\to2)} N_{A,s\text{-}s}^{|1\rangle}} = \frac{k_{A,rad}^{2\to0} k_A^{exc(1\to2)}}{(k_A^{1\to0} + k_A^{exc(1\to2)})(k_A^{2\to1} + k_A^{2\to0}) + k_A^{2\to0} k_A^{exc(1\to2)}} \approx \left[\left(\frac{\lambda_P}{hc}\right)\sigma_A^{1\to2}P\right]\tau_{A,obs}^{|1\rangle} k_{A,rad}^{2\to0} \tau_{A,obs}^{|2\rangle} = \eta_A^{up}(\mathrm{ESA})\phi_A \quad (4)$$

The latter two requirements are fulfilled in aromatic molecules that possess low-lying long-lived triplet states that could be used as intermediate excited relays (level $|1\rangle$ in Figure 3a) and strongly emissive singlet excited states of higher energy (level $|2\rangle$ in Figure 3a). However, the minor spin−orbit coupling constants characterizing light H, C, N, O, P, and S atoms preclude the direct feeding of the long-lived intermediate triplet excited state from the singlet ground state by light excitation. A clever bypass, known as the triplet−triplet annihilation (TTA) upconversion process was first reported during the early 1960s, and it has been optimized during the last two decades to reach remarkable 16−26% intrinsic upconversion quantum yields.[19,20] However, the TTA mechanism requires the diffusion and collision of two excited triplet acceptors, which limits this methodology to intermolecular processes occurring in solution, rubbery polymeric materials, or solid matrices under anaerobic conditions since dioxygen can easily quench triplet excited states. It therefore does not fit the criteria for being considered as a discrete molecular process *stricto sensu* and will not be further discussed here.

The second obvious choice for implementing upconversion using linear optics relies on open-shell d-block (d^n, $n = 1-9$) and f-block metals (f^n, $n = 1-13$), for which the interelectronic repulsions within the frame of the Russell−Saunders coupling scheme produce series of more or less regularly spaced atomic terms (maximum 15 excited terms for the d^5 configuration, but up to 118 excited terms for the f^7 configuration) covering the infrared to X-ray spectral range.[21] When open-shell d-block,[22] or preferably 4f-block,[8] cations are doped into ionic crystals[5,8] or nanoparticles[23] possessing only low-phonon vibrations, the nonradiative relaxation pathways are limited to such an extent that the lifetimes of the crucial excited relays $\tau_{A,obs}^{|1\rangle} = (k_A^{1\to0})^{-1}$ can reach several hundreds of microseconds or even a few milliseconds, so ESA (Figure 4a) can compete favorably with nonradiative relaxation to reach upconverted quantum yields in the 5−10% range (eq 4).[23] However, the presence of closely spaced open-shell metallic centers in bulk materials offers a multitude of possible intermetallic sensitizer/activator energy transfers, which are responsible for more efficient linear upconversion processes gathered under the terms of cross-relaxation (CR), when the acceptor and sensitizer correspond to the same type of metal (Figure 4b),[24] or energy transfer upconversion (ETU), when the sensitizer and the acceptor are of different nature (Figure 4c).[8] The associated set of differential equations is collected in Figure 4d where the second-order rate constants for energy transfers $W_{S\to A}$ obey Fermi's golden rule given in eq 5.[8]

$$W_{S\to A} = \frac{2\pi}{\hbar}|\langle\Psi_S^0\Psi_A^*|H|\Psi_S^*\Psi_A^0\rangle|^2\Omega_{S,A} \quad (5)$$

The wave functions are simple products of single ion wave functions, ψ_S and ψ_A; H is the interaction Hamiltonian that mediates energy transfer from the excited sensitizer S* to the ground-state acceptor A. The interaction mechanism in ionic solids is usually multipolar electrostatic or magnetic,[25] but it can be an exchange coupling when S and A are bridged by a molecular or atomic unit.[26] $\Omega_{S,A}$ is the spectral overlap integral between the sensitizer and the activator, which ensures energy conservation. The ETU mechanism proved to be 2−3 orders of magnitude more efficient than ESA[8] and the first IR → blue upconversion reported for a doped solid in 1966 indeed exploited the $Yb^{3+}(S)/Tm^{3+}(A)$ couple and a 3-photon ETU process.[27] Solving the set of differential equations for steady-state $dN_S^{|i\rangle}/dt = 0$ and $dN_A^{|i\rangle}/dt = 0$ produced by continuous irradiation of the sensitizer S gives eqs 6 and 7, which are strictly identical to eqs 2 and 3 derived for the ESA mechanism if the activator centered absorption rate constants, $k_A^{exc(0\to1)}$ and $k_A^{exc(1\to2)}$, in ESA are replaced with the indirect sensitization pathways, $W_{S\to A}^1 N_{S,s\text{-}s}^{|1\rangle}$ and $W_{S\to A}^2 N_{S,s\text{-}s}^{|1\rangle}$, in ETU, respectively ($N_{S,s\text{-}s}^{|1\rangle}$ is given in eq 8).

$$N_{A,s\text{-}s}^{|1\rangle}(\mathrm{ETU}) = \frac{W_{S\to A}^1 N_{S,s\text{-}s}^{|1\rangle}(k_A^{2\to1} + k_A^{2\to0})}{k_A^{1\to0}(k_A^{2\to1} + k_A^{2\to0}) + k_A^{2\to0} W_{S\to A}^2 N_{S,s\text{-}s}^{|1\rangle}} N_{A,s\text{-}s}^{|0\rangle} \approx \left[\left(\frac{\lambda_P}{hc}\right)\sigma_S^{0\to1}P\right] W_{S\to A}^1 \tau_{S,obs}^{|1\rangle}\tau_{A,obs}^{|1\rangle} N_A^{tot} N_S^{tot} \quad (6)$$

$$N_{A,s\text{-}s}^{|2\rangle}(\mathrm{ETU}) = \frac{W_{S\to A}^1 W_{S\to A}^2 (N_{S,s\text{-}s}^{|1\rangle})^2}{k_A^{1\to0}(k_A^{2\to1} + k_A^{2\to0}) + k_A^{2\to0} W_{S\to A}^2 N_{S,s\text{-}s}^{|1\rangle}} N_{A,s\text{-}s}^{|0\rangle} \approx \left[\left(\frac{\lambda_P}{hc}\right)\sigma_S^{0\to1}P\right]^2 W_{S\to A}^1 W_{S\to A}^2 (\tau_{S,obs}^{|1\rangle})^2 \tau_{A,obs}^{|1\rangle}\tau_{A,obs}^{|2\rangle} N_A^{tot} (N_S^{tot})^2 \quad (7)$$

with

$$N_{S,s\text{-}s}^{|1\rangle}(\mathrm{ETU}) = \frac{k_S^{exc(1\to0)}}{k_S^{1\to0} + W_{S\to A}^1 N_{A,s\text{-}s}^{|0\rangle} + W_{S\to A}^2 N_{A,s\text{-}s}^{|1\rangle}} N_{S,s\text{-}s}^{|0\rangle} = \left[\left(\frac{\lambda_P}{hc}\right)\sigma_S^{0\to1}P\right]\tau_{S,obs}^{|1\rangle} N_{S,s\text{-}s}^{|0\rangle} \quad (8)$$

The dispersive term, $k_A^{2\to0} W_{S\to A}^2 N_{S,s\text{-}s}^{|1\rangle}$, responsible for saturation at high excitation intensity, can be neglected under reasonable continuous illumination of the sensitizer. The major fractions of the sensitizers and activators remain thus in the ground state ($N_{A,s\text{-}s}^{|0\rangle} \simeq N_A^{tot}$ and $N_{S,s\text{-}s}^{|0\rangle} \simeq N_S^{tot}$), so eqs 6 and 7 can be simplified where $\tau_{X,obs}^{|i\rangle} = (\sum_j k_{X,obs}^{i\to j})^{-1}$ is the characteristic excited-state lifetime of level $|i\rangle$ located on the X center.

The associated ETU upconversion quantum yield, $\phi_A^{up}(\mathrm{ETU})$ is defined in the first line of eq 9. Under reasonable illumination regime, it can be developed to give the two last lines in eq 9.[3]

$$\phi_A^{up}(\mathrm{ETU}) = \frac{\text{emitted photons}}{\text{absorbed photons}} = \frac{k_{A,rad}^{2\to0} N_{A,s\text{-}s}^{|2\rangle}}{k_S^{exc(0\to1)} N_{S,s\text{-}s}^{|0\rangle}} \approx \left[\left(\frac{\lambda_P}{hc}\right)\sigma_S^{0\to1}P\right] W_{S\to A}^1 W_{S\to A}^2 (\tau_{S,obs}^{|1\rangle})^2 \tau_{A,obs}^{|1\rangle} N_A^{tot} N_S^{tot} k_{A,rad}^{2\to0}\tau_{A,obs}^{|2\rangle} = \eta_{S,A}^{up}(\mathrm{ETU})\phi_A \quad (9)$$

Compared with $\phi_A^{up}(\mathrm{ESA})$ in eq 4, one notes that $\phi_A^{up}(\mathrm{ETU})$ in eq 9 benefits from the replacement of the activator absorption cross section ($\sigma_A^{1\to2}$) with that of the sensitizer $\sigma_S^{0\to1}$, which is

https://doi.org/10.1021/acs.accounts.1c00685
Acc. Chem. Res. 2022, 55, 442−456

prone to be enhanced. The additional terms, $W^{1}_{S\to A}W^{2}_{S\to A}(\tau^{|1\rangle}_{S,obs})^2$, open some perspectives for optimizing ETU. One notes that the ultimate dependence of ϕ^{up}_{A}(ETU) on the concentrations of both activators and sensitizers in $\eta^{up}_{S,A}$(ETU) results from the operation of second-order energy transfer rate constants, which imply "associated" intermolecular SA pairs for inducing upconversion in doped solids. Despite the obvious larger possibilities brought by ETU in terms of tuning and optimization, the complicated statistical modeling of second-order energy transfer rate constants pertinent to doped solids or nanoparticles severely limits predictions and rational design.[26,28] Moreover, the recent need for applications of microscopic upconversion nanoparticles as near-infrared imaging probes for biological tracing and for medical diagnosis is currently hindered by surface quenching, difficult reproducibility, and biological clearance inherent to ionic solids. The induction of linear upconversion into isolated (supra)molecular complexes therefore represents a breakthrough in terms of mechanism because the intermolecular energy transfers required for crucial cross-relaxation and photon avalanche processes operating in bulk materials are difficult to implement into molecules (Figure 4b).[2,18,29,30] On the other side, the excited state absorption mechanism (ESA, Figure 4a) is fully adapted for working in isolated molecules, but recent efforts discussed below made energy transfer upconversion (ETU), cooperative luminescence (CL), and cooperative upconversion (CU) also compatible with their accomplishment in isolated molecules (Figure 5).

2. LINEAR LIGHT UPCONVERSION IMPLEMENTED IN MONONUCLEAR MOLECULAR COMPLEXES: THE EXCITED-STATE ABSORPTION (ESA) MECHANISM

At the turn of the century, Reinhard and Güdel focused their attention on molecular systems with the NIR excitation (780−950 nm) of triple-helical $[Ln(DPA)_3]^{3-}$ complexes using a tunable Ti-sapphire laser source (Ln = Er^{3+}, Tm^{3+} Yb^{3+}; Figure 6a, left).[31] Beyond the expected downshifted emission detected for Ln = Tm, Yb according to the antenna effect, no upconverted signal could be detected. These authors concluded that the short excited-state lifetimes characterizing these molecular compounds ($\tau^{|1\rangle}_{A,obs} \leq 1\ \mu s$) allowed no chance to induce and observe upconversion luminescence.[31] Switching from a "timid" continuous-wave Ti-sapphire source ($P_{max} \approx 1-10\ W{\cdot}cm^{-2}$)[31] to highly focused coincident 10 ns laser pulses with peak powers near 100 kW ($P > 10^9\ W{\cdot}cm^{-2}$)[32] compensates for any short intermediate $\tau^{|1\rangle}_{A,obs}$ excited lifetimes in eq 4, and aqueous solutions of $[Ln(DPA)_3]^{3-}$ (Ln = Er, Tm) finally displayed weak NIR to visible light upconversion upon dual massive laser pump excitations (Figure 6, left).

A similar approach used a near-infrared OPO tunable femtosecond laser focused on $Tm(CF_3SO_3)_3$ dissolved in DMSO-d_6 (Figure 6, right).[33] Thorough analysis of the excitation spectrum responsible for the upconverted 480 nm $Tm(^1G_4 \to {}^3H_6)$ luminescence shows a major peak corresponding to two-photon NLO absorption ($^1G_4 \leftarrow {}^3H_6$ at λ_{exc} = 950 nm) and a weak shoulder assigned to a competitive linear ESA upconversion process at λ_{exc} = 790 nm (Figure 7, right).[33] Under such large pump intensities, ultraweak NLO processes become accessible to detection[34] and compete with the weak linear ESA mechanism operating in nonoptimized molecular complexes.

In an effort to increase the intermediate excited-state lifetime $\tau^{|1\rangle}_{A,obs}$ via the protection of the metallic lanthanide center from interactions with high-energy oscillators of the ligands or of close

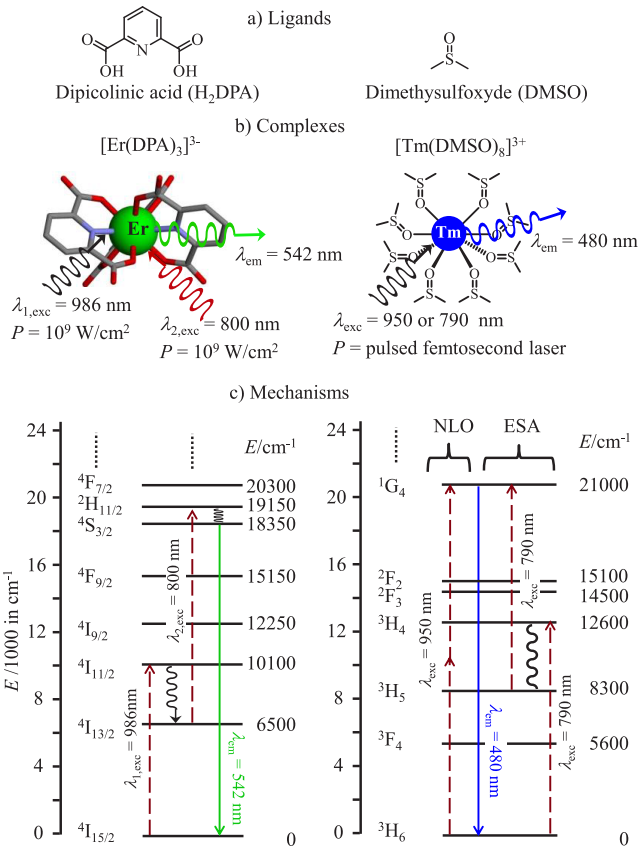

Figure 6. NIR to visible light upconversion assigned to the ESA mechanism and observed under massive excitation power intensities operating for $[Er(DPA)_3]^{3-}$ in water (data from ref 32) and $Tm(CF_3SO_3)_3$ in DMSO-d_6 (data from ref 33).

solvent molecules, Charbonnière and co-workers suggested that a single-center ESA mechanism could be responsible for the upconverted visible signal detected for monomeric [Er(I-DOTA)F] units in deuterated water upon reasonable excitation intensities (around 10 $W{\cdot}cm^{-2}$ at 980 nm, Figure 7).[35] The presence of protecting fluoride anions to saturate the erbium coordination sphere probably contributes to the ultimate multiple visible upconversion luminescence.[35]

A deliberate design of molecular complexes programmed for single-center ESA light upconversion under reasonable excitation intensities can be traced back to the synthesis of triple-stranded erbium complexes with polyaromatic tridentate ligands **L** possessing increased complexities and sizes (Figure 7a).[3,36−38] The resulting triple-helical complexes $[Er(DPA)_3]^{3-}$, $[ErL_3]^{3+}$ (L = DPA-R, R-tpy, and R-bzimpy), and $[GaErGa(dipy-bzimpy)_3]^{9+}$ (Figure 7b) are quantitatively formed in acetonitrile at millimolar concentrations[36] and display dual downshifted microsecond infrared $Er(^4I_{13/2} \to {}^4I_{15/2})$ emissions at 1520−1540 nm ($\tau^{|1\rangle}_{Er,obs} \approx 2-6\ \mu s$, Figure 8a,b) and nanosecond visible $Er(^4S_{3/2} \to {}^4I_{15/2})$ emission at 542 nm ($\tau^{|2\rangle}_{Er,obs} \approx 38-40$ ns, Figure 8a) under standard ligand excitation.[3,37,38] Upon near-infrared excitation of the $Er(^4I_{9/2} \leftarrow {}^4I_{15/2})$ transition at 801 nm and using P = 3−25 $W{\cdot}cm^{-2}$, all these complexes display the expected one-photon downshifted infrared $Er(^4I_{13/2} \to {}^4I_{15/2})$ band at 1520−1540 nm, together with two-photon upconverted green $Er(^4S_{3/2} \to {}^4I_{15/2})$ luminescence with low, but structurally tunable quantum yields at room temperature in acetonitrile ($5.5 \times 10^{-11} \leq \phi^{up}_{A}(ESA) \leq 1.7 \times 10^{-9}$ at P = 25 $W{\cdot}cm^{-2}$, Figures 7b and 8c).[3,37,38] Having $k^{2\to 0}_{A,rad}$, P, $\tau^{|1\rangle}_{Er,obs}$, $\tau^{|2\rangle}_{Er,obs}$, and ϕ^{up}_{A}(ESA) in

https://doi.org/10.1021/acs.accounts.1c00685
Acc. Chem. Res. 2022, 55, 442−456

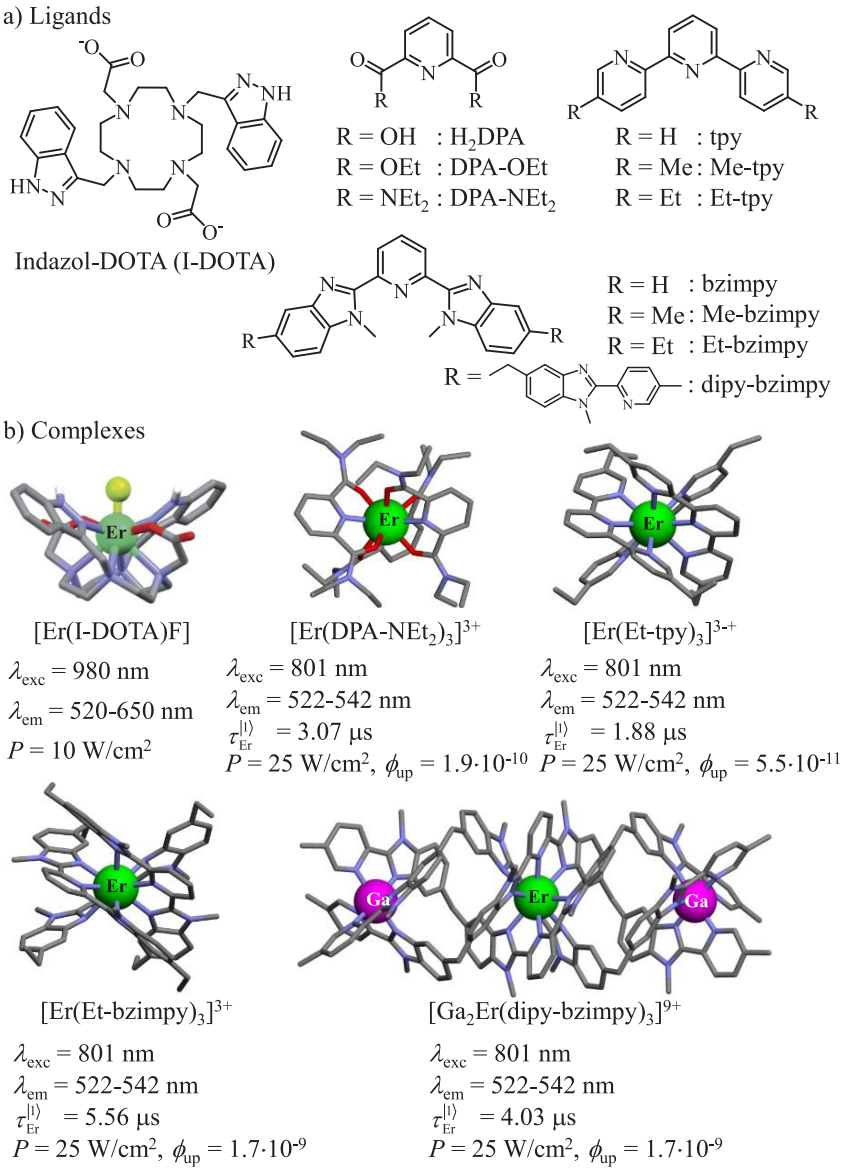

Figure 7. NIR to visible light upconversion assigned to the ESA mechanism and observed under reasonable excitation intensities for [Er(I-DOTA)F] in D_2O (data from ref 35), $[Er(DPA)_3]^{3-}$, $[ErL_3]^{3+}$ (L = DPA-R, R-tpy), and $[GaErGa(dipy\text{-}bzimpy)_3]^{9+}$ in acetonitrile, data from refs 3 and 36−38).

hand, eq 4 gives access to the intrinsic erbium-centered luminescence quantum yields, $\phi_{Er} = k^{2\rightarrow 0}_{Er,rad}\tau^{|2\rangle}_{Er,obs}$, and to $\eta^{up}_{Er}(ESA) = \phi^{up}_{Er}(ESA)/\phi_{Er} = [(\lambda_p/hc)\sigma^{1\rightarrow 2}_{Er}P]\tau^{|1\rangle}_{Er,obs}$, from which the nonexperimentally accessible absorption cross sections $\sigma^{1\rightarrow 2}_{Er}$ of the Er($^2H_{11/2}$, $^4S_{3/2} \leftarrow {}^4I_{13/2}$) ESA process can be deduced (Figure 8c).[3] The associated decadic absorption coefficients $\varepsilon^{1\rightarrow 2}_{Er} = (2.6 \times 10^{20})\sigma^{1\rightarrow 2}_{Er}$ cover the 1−50 $M^{-1}\cdot cm^{-1}$ range and exceed by at least 2 orders of magnitude the efficiency of the Er($^4I_{9/2} \leftarrow {}^4I_{15/2}$) ground-state absorption (GSA) process ($0.07 \leq \varepsilon^{0\rightarrow 1}_{Er} \leq 0.12\ M^{-1}\cdot cm^{-1}$). The occurrence of this phenomenon is supported by SO-CASSCF calculations and tentatively assigned to minor covalent mixing between the excited states of the metals and those of the bound aromatic ligands.[3]

3. LINEAR LIGHT UPCONVERSION IMPLEMENTED IN MOLECULAR COMPLEXES: THE ENERGY TRANSFER UPCONVERSION (ETU) MECHANISM

Despite the drastic reduction of the lifetimes of intermediate excited states in molecules, which control the quantum yields of the ETU mechanism ($(\tau^{|1\rangle}_{S,obs})^2\tau^{|1\rangle}_{A,obs}$ in eq 9), massive NIR excitation of ytterbium sensitizers at 980 nm ($^2F_{5/2} \leftarrow {}^2F_{7/2}$) led to detectable upconverted visible Er($^4S_{3/2} \rightarrow {}^4I_{15/2}$) activator-based emission at 540 nm in statistically doped Yb/Er lanthanide coordination polymers.[39−41] Attempts to prepare discrete molecular entities displaying upconversion using ETU or CR mechanisms can be traced back to the suggested formation of (i) ionic [IR-806][$Er(tta)_4$] pairs in nonpolar organic solvents (Figure 9a)[42] and (ii) fluoro-bridged $\{[Er(I\text{-}DOTA)]_2F\}^+$ dimers in water (Figure 9b).[35] This strategy has been extended in materials science where polynuclear lanthanide complexes are statistically doped with ytterbium (S) and erbium (A), while yttrium is used as a "diluting" cation either in the solid state[43] or in solution.[44]

Interestingly, the discrete $[CrErCr(dipy\text{-}pybzimpy)_3]^{9+}$ complex, which corresponds to the first report in 2011 of a planned molecular-based upconversion induced under reasonable excitation intensities, exploits the ETU mechanism (Figure 10a).[45] It implies the operation of two successive chromium to

https://doi.org/10.1021/acs.accounts.1c00685
Acc. Chem. Res. 2022, 55, 442−456

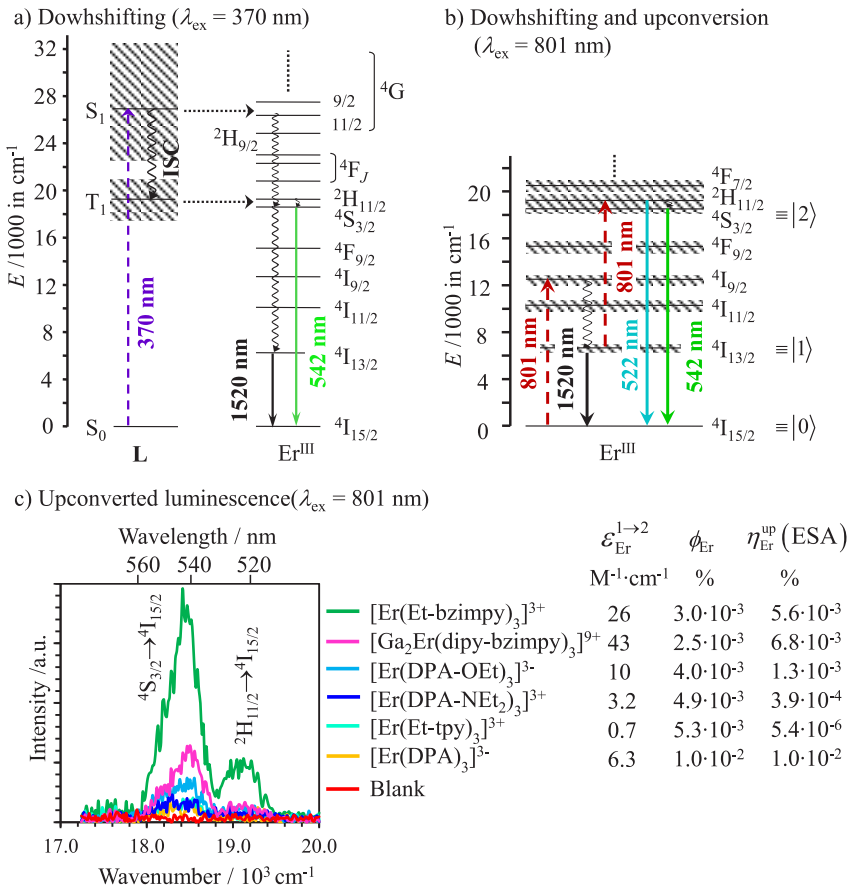

	$\varepsilon_{Er}^{1\to2}$ $M^{-1}\cdot cm^{-1}$	ϕ_{Er} %	η_{Er}^{up}(ESA) %
$[Er(Et\text{-}bzimpy)_3]^{3+}$	26	$3.0\cdot10^{-3}$	$5.6\cdot10^{-3}$
$[Ga_2Er(dipy\text{-}bzimpy)_3]^{9+}$	43	$2.5\cdot10^{-3}$	$6.8\cdot10^{-3}$
$[Er(DPA\text{-}OEt)_3]^{3-}$	10	$4.0\cdot10^{-3}$	$1.3\cdot10^{-3}$
$[Er(DPA\text{-}NEt_2)_3]^{3+}$	3.2	$4.9\cdot10^{-3}$	$3.9\cdot10^{-4}$
$[Er(Et\text{-}tpy)_3]^{3+}$	0.7	$5.3\cdot10^{-3}$	$5.4\cdot10^{-6}$
$[Er(DPA)_3]^{3-}$	6.3	$1.0\cdot10^{-2}$	$1.0\cdot10^{-2}$

Figure 8. Jablonski diagrams summarizing the optical processes operating in the triple-helical complexes $[ErL_3]^{3+}$ and $[Er(DPA)_3]^{3-}$ upon (a) ligand-centered (λ_{ex} = 370 nm) and (b) erbium-centered (λ_{ex} = 801 nm) excitation. (c) Upconverted visible $Er(^2H_{11/2} \to {}^4I_{15/2})$ and $Er(^4S_{3/2} \to {}^4I_{15/2})$ emission spectra observed for $[ErL_3]^{3+}$, $[GaErGaL_3]^{9+}$, and $[Er(DPA)_3]^{3-}$ upon laser excitation of the $Er(^4I_{9/2} \leftarrow {}^4I_{15/2})$ transition at λ_{exc} = 801 nm and using incident pump intensity P = 25 W·cm^{-2} in acetonitrile solution at 298 K. The calculated ESA absorption coefficients, $\varepsilon_{Er}^{1\to2}$, intrinsic quantum yields, $\phi_{Er} = k_{Er,rad}^{2\to0}\tau_{Er,obs}^{|2\rangle}$, and ESA efficiencies, $\eta_{Er}^{up}(ESA) = k_{Er}^{exc(1\to2)}/k_{Er,obs}^{1\to0} = [(\lambda_p/hc)\sigma_A^{1\to2}P]\tau_{A,obs}^{|1\rangle}$, are highlighted (data from ref 3).

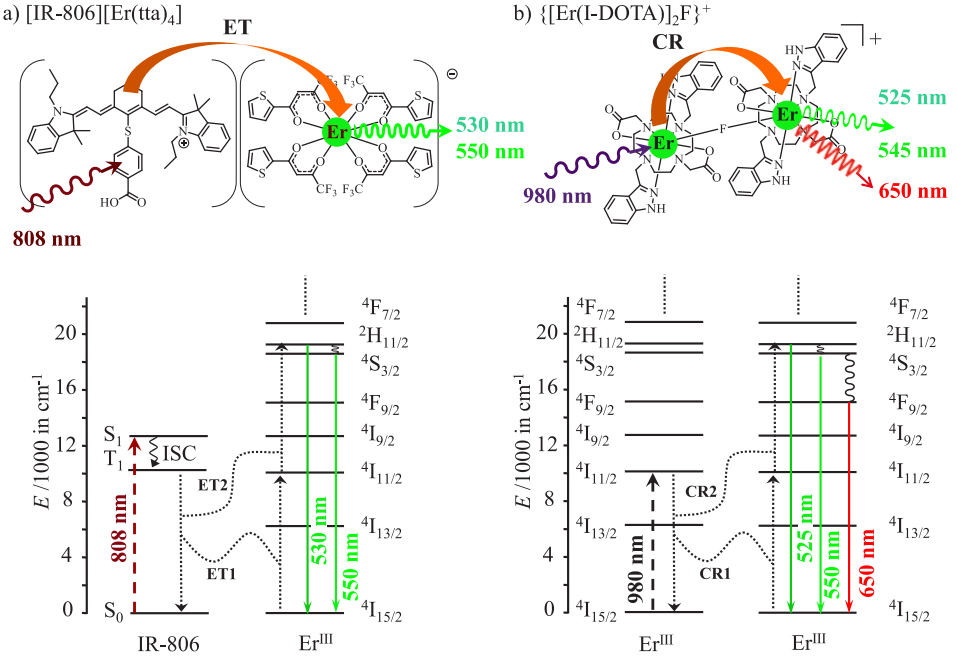

Figure 9. NIR to visible light upconversion observed under reasonable excitation power intensities and assigned to the ETU mechanism for (a) [IR-806][Er(tta)$_3$] ion pairs in dichloromethane (data from ref 42) and (b) $\{[Er(I\text{-}DOTA)]_2F\}^+$ dimers in water (data from ref 35).

https://doi.org/10.1021/acs.accounts.1c00685
Acc. Chem. Res. 2022, 55, 442−456

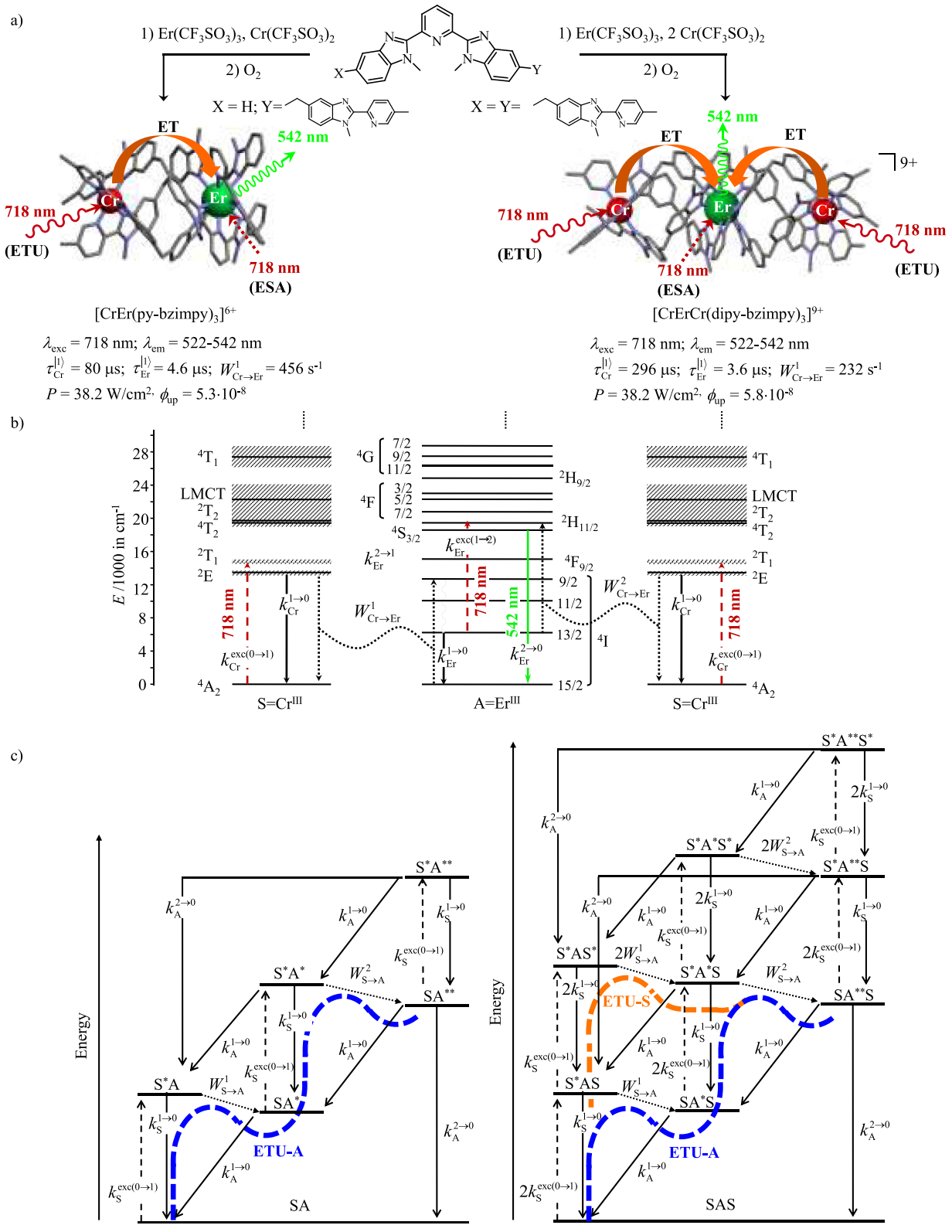

Figure 10. (a) NIR to visible light upconversion observed under reasonable excitation power intensities (measured in acetonitrile at RT) operating in discrete self-assembled $[CrEr(py\text{-}bzimpy)_3]^{6+}$ and $[CrErCr(dipy\text{-}pybzimpy)_3]^{9+}$, (b) Jablonski diagram highlighting the competitive ETU and ESA mechanisms, and (c) associated kinetic diagrams (data from refs 3, 45, and 46).

erbium energy transfers characterized by first-order rate constants, $W^1_{S\to A}$ and $W^2_{S\to A}$ (Figure 10b) modeled with Fermi's golden rule given in eq 10.[47]

$$W_{S\to A} = \frac{2\pi}{\hbar}\,|\langle \Psi_{SA^*}|H|\Psi_{S^*A}\rangle|^2 \Omega_{S,A} \tag{10}$$

Compared with second-order rate constants pertinent to ETU mechanisms implemented in doped macroscopic materials (eq

https://doi.org/10.1021/acs.accounts.1c00685
Acc. Chem. Res. 2022, 55, 442−456

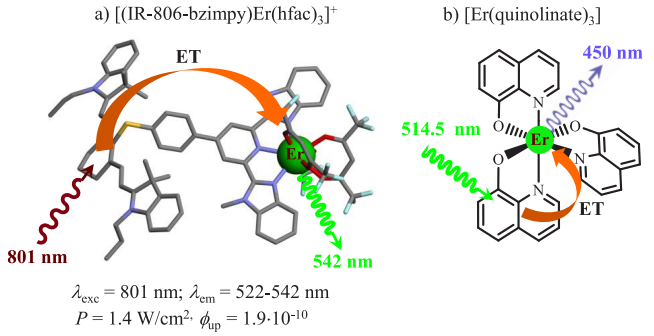

Figure 11. Linear light upconversion assigned to the ETU mechanism and observed under reasonable excitation intensity powers in (a) molecular $[(\text{IR-806-bzimpy})\text{Er(hfac)}_3]^+$ in acetonitrile (data from ref 4) and (b) thin films containing $[\text{Er(quinolinate)}_3]$ (data from ref 48).

5), the first-order character of intramolecular energy transfers, $W_{S\to A}$, operating in molecules (eq 10) removes the dependence of the upconverted quantum yield $\phi_A^{up}(\text{ETU})$ on the concentration of the activator and of the sensitizer because the kinetic differential equations do not contain anymore sensitizer/activator cross terms of the type $W_{S\to A}^1 N_S^{|1\rangle} N_A^{|0\rangle}$ or $W_{S\to A}^2 N_S^{|1\rangle} N_A^{|1\rangle}$ (Figure 4d). With this in mind. the steady-state populations obtained under continuous excitation can be predicted with the help of simple matrix inversion methods[1] applied to the kinetic diagrams established for S_nA molecular systems (Figure 10c).[46] For the simplest case of a S/A pair found in $[\text{CrEr(pybzimpy)}_3]^{6+}$ (S = Cr, A = Er),[1] the efficiency of the ETU mechanism (blue trace in Figure 10c, left) critically depends on the adverse competition between the second sensitizer-based excitation process $k_{Cr}^{exc(0\to1)}$ (on the order of 0.015 s^{-1} for $P = 38.2$ $W\cdot cm^{-2}$ since $\varepsilon_{Cr}^{0\to1} = 0.03$ $M^{-1}\cdot cm^{-1}$, eq 1) and the relaxation rate constants of the intermediate activator-based excited state $k_{Er}^{1\to0}$ (on the order of 2×10^5 s^{-1}).[3] The predicted upconverted quantum yield of $\phi_{up}(\text{ETU}) \approx 3 \times 10^{-15}$ at $P = 38.2$ $W\cdot cm^{-2}$ is therefore negligible and 6 orders of magnitude lower than $\phi_{up}(\text{ESA}) = 1.7 \times 10^{-9}$ reported for ESA operating in the isolated activator $[\text{Er(Et-bzimpy)}_3]^{3+}$ at $P = 25$ $W\cdot cm^{-2}$ (Figure 7).[3] The situation can be improved when the poor $[\text{Cr(III)N}_6]$ sensitizer embedded in $[\text{CrEr(py-bzimpy)}_3]^{6+}$ is replaced with a NIR-absorbing cyanine dye, which boosts $k_S^{exc(0\to1)}$ to reach 1.35×10^5 s^{-1} in $[(\text{IR-806-bzimpy})\text{Er(hfac)}_3]^+$ ($\varepsilon_{IR\text{-}806}^{0\to1} = 230\,000$ $M^{-1}\cdot cm^{-1}$ at $\lambda_{exc} = 801$ nm, Figure 11a).[4] This strategy is reminiscent of a claim for a detectable 514.5 to 450 nm upconversion process obtained upon laser excitation of a poorly characterized organometallic film containing $[\text{Er(quinolinate)}_3]$ complexes (Figure 11b).[48]

Beyond the statistical gain $n^2 = 2^2 = 4$ due to the presence of two Cr(III) sensitizers per erbium activator in [CrErCr(dipy-

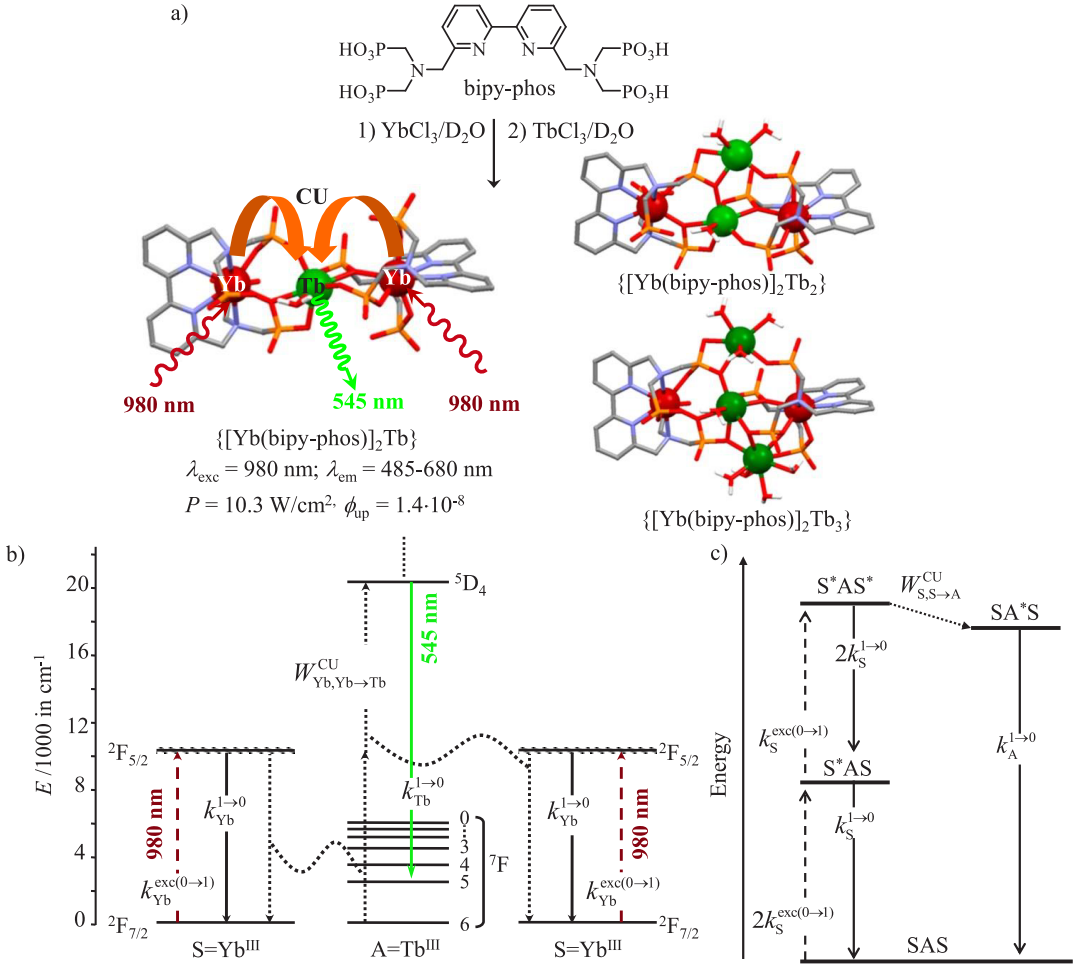

Figure 12. (a) NIR to visible light upconversion observed under reasonable excitation power intensities (measured in D_2O at *RT*) for discrete self-assembled $\{[\text{Yb(bipy-phos)}]_2\text{Tb}_x\}$ ($x = 1-3$, data from ref 50), (b) Jablonski diagram highlighting the CU mechanisms (cooperative upconversion, dotted arrows), and (c) associated kinetic diagram.

https://doi.org/10.1021/acs.accounts.1c00685
Acc. Chem. Res. 2022, 55, 442−456

bzimpy)$_3$]$^{9+}$ (blue trace in Figure 10c. right), the possibility of accumulating photons on the sensitizer prior to undergoing S → A energy transfers may significantly boost the global upconversion when using long-lived sensitizers (orange trace in Figure 10c, right). ϕ_{up}(ETU) ≈ 2 × 10^{-13} at P = 38.2 W·cm^{-2} can be theoretically predicted for [CrErCr(dipy-bzimpy)$_3$]$^{9+}$ in acetonitrile at room temperature, a quantum yield 2 orders of magnitude larger than that expected for [CrEr(py-bzimpy)$_3$]$^{6+}$.[3] The experimental upconversion quantum yields ϕ_{up} ≈ 5.3 × 10^{-8} for [CrEr(py-bzimpy)$_3$]$^{6+}$ and 5.8 × 10^{-8} for [CrErCr-(dipy-bzimpy)$_3$]$^{9+}$ recorded in acetonitrile at P = 38.2 W·cm^{-2} (Figure 10a)[3] greatly exceed the theoretical predictions and are even 2 orders of magnitude larger than that measured for the optimized dye-sensitized upconversion operating in [(IR-806-bzimpy)]Er(hfac)$_3$]$^+$ (Figure 11a). The key to the problem lies in the competition with the ESA mechanism, which is able to overcome the inefficient second Cr-based sensitizing process via competition with an efficient CrEr* → CrEr** excited-state absorption (highlighted with red dotted arrows in Figure 10b).[3]

4. LINEAR LIGHT UPCONVERSION IMPLEMENTED IN MOLECULAR COMPLEXES: THE COOPERATIVE UPCONVERSION (CU) MECHANISM

The cooperative upconversion mechanisms (pertinent to absorption or to simultaneous emission) involve two-center optical transitions, which have nonzero radiative dipole moment matrix elements only when the electrons of the two centers are close enough to significantly interact so that their initial (sa) and final ($s'a'$) states are adequately modeled by the ion-pair wave functions $\Psi^0_{SA,pair}$ (eq 11) and $\Psi'_{SA,pair}$ (eq 12) corrected to first-order for their electrostatic interactions.[49]

$$\Psi^0_{SA,pair} = |sa\rangle - \sum_{s''\neq 0}\sum_{a''\neq 0} \frac{\langle s''a''|H_{SA}|sa\rangle}{\delta_{s''} + \delta_{a''}}|s''a''\rangle \quad (11)$$

$$\Psi'_{SA,pair} = |s'a'\rangle - \sum_{s''\neq s'}\sum_{a''\neq a'} \frac{\langle s''a''|H_{SA}|s'a'\rangle}{\delta_{s''} - \delta_{s'} + \delta_{a''} - \delta_{a'}}|s''a''\rangle \quad (12)$$

Here $s''a''$ denote intermediate states for centers S and A and δ_i represent to their corresponding energies. The double-operator nature of cooperative upconversion (CU) processes limits their efficiency by several orders of magnitude with respect to ETU, and the CU mechanisms have to be considered practically only when ETU cannot take place.[8] Consequently, CU becomes interesting for sensitizing the trivalent lanthanide cations Eu^{3+}, Gd^{3+}, and Tb^{3+}, which display impressive intrinsic visible Eu($^5D_0 \rightarrow {}^7F_J$) and Tb($^5D_4 \rightarrow {}^7F_J$) and UV Gd($^6P_{7/2} \rightarrow {}^8S_{7/2}$) emission quantum yields, but for which there is no available intermediate excited relay between the ground and emissive multiplets compatible with ETU mechanisms.[5]

At the molecular level, Charbonnière and co-workers were the first to combine Yb^{3+} sensitizers and Tb^{3+} activators in what is proposed to be a step-by-step coordination mechanism with no metal scrambling to give well-defined {[Yb(bipy-phos)]$_2$Tb$_x$} complexes in deuterated water (x = 1−3; Figure 12a).[50] Laser excitation of the Yb($^2F_{5/2} \leftarrow {}^2F_{7/2}$) transition at 980 nm indeed induced visible Tb($^5D_4 \rightarrow {}^7F_J$) ($J$ = 1−5) emission covering the 485−680 nm range. The two-photon upconversion mechanism can be only explained by cooperative upconversion (Figure 12b).[51]

The remarkable overall upconversion quantum yield ϕ_{up}(CU) = 1.4 × 10^{-8} at P = 10.3 W·cm^{-2} measured for {[Yb(bipy-phos)]$_2$Tb$_x$} in D_2O compares well with that reported for ETU mechanisms exploiting erbium activators (Figure 10a). The replacement of the erbium activator ($\phi^{^4S_{3/2}\rightarrow {}^4I_{15/2}}_{intrinsic} \approx 10^{-5}$) with its terbium counterpart ($\phi^{^5D_4\rightarrow {}^7F_J}_{intrinsic} \approx 0.5$) in molecular complexes eventually compensates for the expected weak efficiency of the second-order perturbation CU mechanism.[3] This strategy has been successfully repeated for a mixture of {[Yb(TACN-phos)]$_2$Tb$_x$} in deuterated water (x = 1, 2; ϕ_{up}(CU) = 1.4 × 10^{-8} at P = 2.86 W·cm^{-2}; Figure 13a).[52−54] Upconversion could be also induced in light water, and it reached ϕ_{up}(CU) = 1 × 10^{-7} at P = 2.86 W·cm^{-2} in the statistically doped nonanuclear cluster {[Yb$_8$Tb-(acac)$_{16}$(OH)$_{10}$]OH (Figure 13b).[55,56]

A few cases of cooperative upconversion (CU) have been reported for solid hybrids materials, for instance, in some poorly characterized ultradried co-doped organic polymers [Yb$_{1-x}$Eu$_x$(PFBS)] where PFBS is perfluorobutanesulfonate,[57] in cocrystallized [Yb**L**$_3$]$_{0.7}$[Tb**L**$_3$]$_{0.3}$ coordination complexes where **L** stands for the didentate perfluoroimidodiphosphinimidate ligands[58] and in the ionic [Yb(dpa)$_3$][Cr(ddpd)$_2$] salt (Figure 14a).[59] A rare case of cooperative luminescence, that is, a cooperative upconversion process where the lack of activator-centered excited relay is replaced by a virtual emissive state,[8] was reported for solids samples of [Yb(dppz)(ttfa)$_3$] undergoing massive femtosecond pulsed laser excitation (Figure 14b).[60]

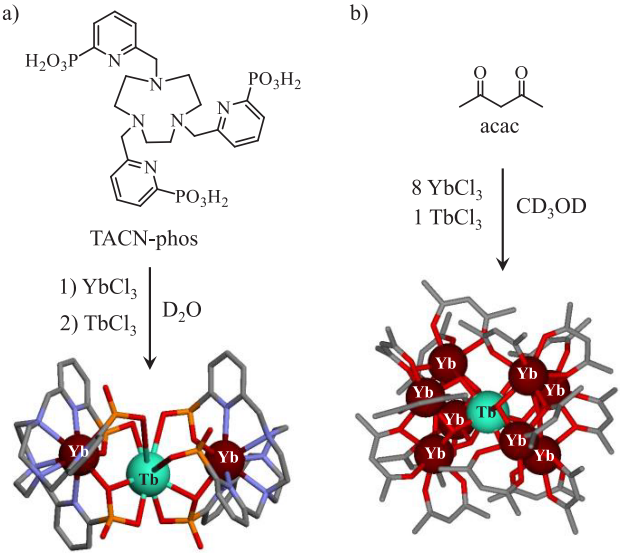

Figure 13. Formation of heterometallic (a) {[Yb(TACN-phos)]$_2$Tb} (data from ref 54) and (b) {[Yb$_8$Tb(acac)$_{16}$(OH)$_{10}$]OH complexes in solution (data from ref 56), which exhibit NIR (980 nm) to visible (485−650 nm) light upconversion according to the cooperative upconversion (CU) mechanism.

https://doi.org/10.1021/acs.accounts.1c00685
Acc. Chem. Res. 2022, 55, 442−456

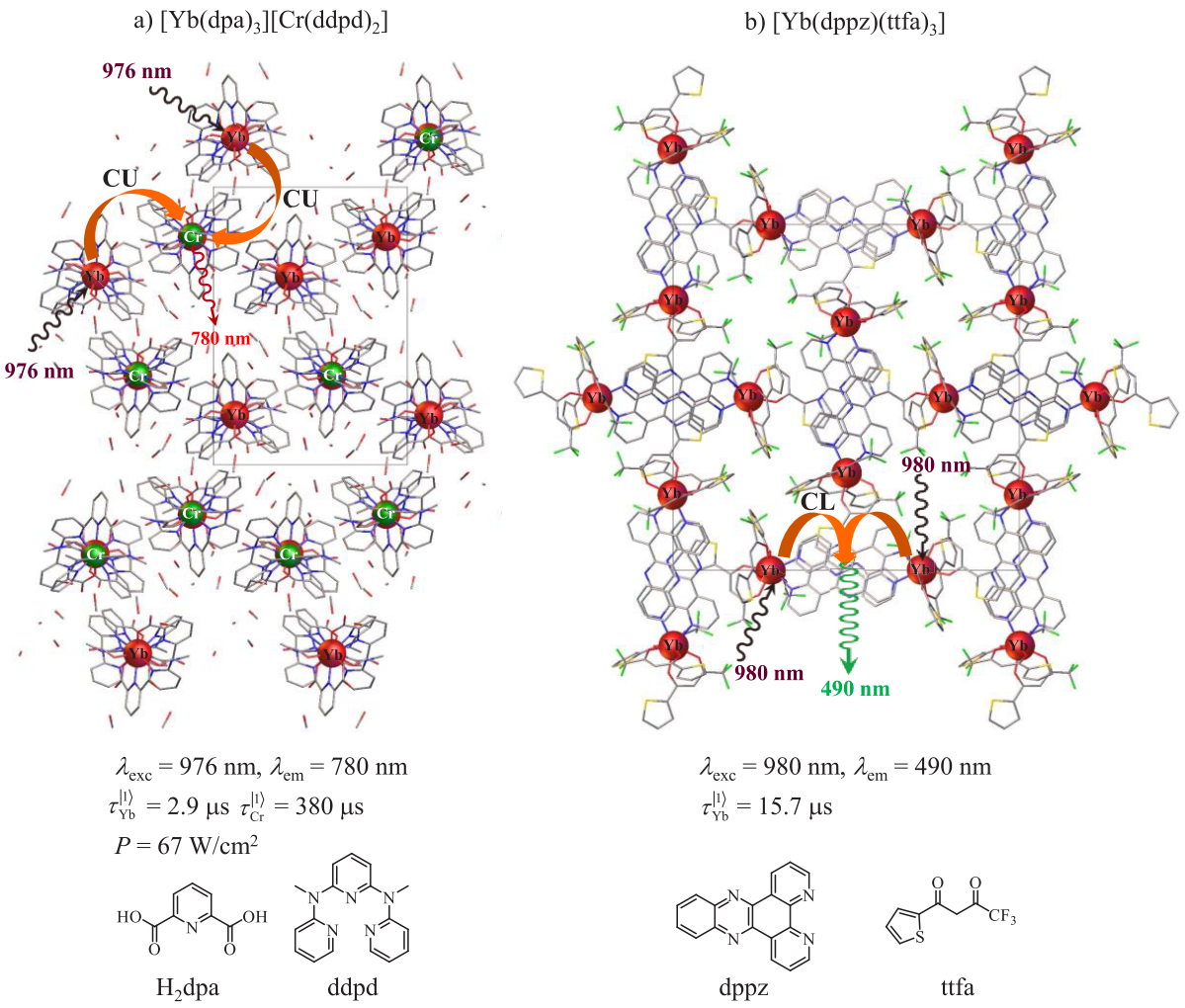

Figure 14. Solid-state crystal structures of (a) $[Yb(dpa)_3][Cr(ddpd)_2]$ (data from ref 59) and (b) $[Yb(dppz)(ttfa)_3]$ (data from ref 60), which exhibit NIR (980 nm) to visible light upconversion according to (a) cooperative upconversion (CU) and (b) cooperative luminescence (CL) mechanisms in the solid state.

5. CONCLUSIONS

Trivalent lanthanides with their scales of well-defined and sometimes long-lived and emissive excited states offer the best perspectives for implementing linear light-upconversion in discrete molecules. The three most common and well-known upconversion mechanisms operating in doped ionic solids, excited-state absorption (ESA), energy transfer upconversion (ETU), and cooperative upconversion (CU), have been successfully implemented in discrete coordination complexes during the past decade. The single-centered ESA mechanism is easy to implement in discrete and isolated molecules, but the dipole-forbidden nature of the intrashell f → f transitions and the short lifetimes of the excited relays severely limit (i) the efficiency of the upconversion process and (ii) the potential applications in biology (luminescent probes) and medicine (disease detection and theranostics).[60] The replacement of high-energy C−H and O−H vibrations with C−F, C−D, and O−D analogues of lower energies in the bound ligands is probably the best cure to overcome these roadblocks and to maximize $\eta_A^{up}(ESA)$.[40,61,62] Moreover, the global upconversion quantum yields $\phi_A^{up}(ESA) = \eta_A^{up}(ESA)\phi_A$ also depends on the ultimate intrinsic quantum yield of the activator ϕ_A, a factor that is drastically limited for lanthanides possessing series of regularly spaced $^{2S+1}L_J$ spectroscopic levels in molecular complexes. The assignment of the sensitization and emission processes to different partners represents a second cure for improving linear upconversion by using the ETU mechanism. Contrary to doped solids where the intermolecular energy transfer processes between the sensitizers and the activators are controlled by second-order kinetic rate laws, the association of the sensitizers and activators in the same molecular unit results in first-order kinetic rate laws that simplify physical modeling, prediction, design, and optimization. This molecular strategy opens remarkable perspectives when pure and well-organized (not statistically doped) heterometallic p−f,[63] d−f,[64,65] and f−f′[66−69] complexes are considered. If p−f pairs have been overexploited in coordination chemistry due to the early recognition of the benefit provided by the antenna effect for sensitizing trivalent lanthanides,[6] the selective assembly of d−f systems is less common but still well-represented because the difference in the stereochemical preferences of well-identified d−f pairs can be exploited. Nonstatistical f−f′ pairs, which are the most promising candidates for molecular-based linear upconversion, remain (very) difficult to prepare in solution. We do believe that the large increase in quantum yield required for molecular upconversion to reach the low-power excitation intensities compatible with practical biological applications could be only obtained if photobleaching-resistant nonstatistical heterometal-

https://doi.org/10.1021/acs.accounts.1c00685
Acc. Chem. Res. 2022, 55, 442−456

lic sensitizer$_n$−acceptor molecular building blocks (S_nA) of f−f type could be designed. The Yb_nEr or Yb_nTb combinations, where the two types of cations are linked by short bridges favoring Dexter energy transfer mechanisms, are among the most promising pairs granting that the metals additionally lie in low-energy phonon environments.[70] This strategy is reminiscent of that followed for optimizing light upconversion operating in nanoparticles, but in molecules, it will benefit from easy reproducibility, optical rationalization, and controlled speciation, a highly desired situation when these probes have to be introduced into complex mixtures pertinent to biology and medicine.

AUTHOR INFORMATION

Corresponding Author

Claude Piguet − *Department of Inorganic and Analytical Chemistry, University of Geneva, CH-1211 Geneva 4, Switzerland;* orcid.org/0000-0001-7064-8548; Email: claude.piguet@unige.ch

Authors

Hélène Bolvin − *Laboratoire de Chimie et Physique Quantiques, CNRS, Université Toulouse III, F-31062 Toulouse, France;* orcid.org/0000-0002-6302-7820

Alexandre Fürstenberg − *Department of Inorganic and Analytical Chemistry and Department of Physical Chemistry, University of Geneva, CH-1211 Geneva 4, Switzerland;* orcid.org/0000-0002-6227-3122

Bahman Golesorkhi − *Department of Inorganic and Analytical Chemistry, University of Geneva, CH-1211 Geneva 4, Switzerland;* orcid.org/0000-0001-8922-3814

Homayoun Nozary − *Department of Inorganic and Analytical Chemistry, University of Geneva, CH-1211 Geneva 4, Switzerland*

Inès Taarit − *Department of Inorganic and Analytical Chemistry, University of Geneva, CH-1211 Geneva 4, Switzerland*

Complete contact information is available at: https://pubs.acs.org/10.1021/acs.accounts.1c00685

Notes

The authors declare no competing financial interest.

Biographies

Hélène Bolvin obtained her Ph.D. degree in 1993 under the supervision of Olivier Kahn. She is currently a senior scientist in quantum chemistry at the University of Toulouse.

Bahman Golesorkhi received a B.Sc. from Shiraz University, Iran, in 2011 and a M.Sc. from Sharif University of Technology, Iran, in 2013. He then moved to the University of Geneva, Switzerland, and obtained his Ph.D. in the field of lanthanide-based upconversion in 2019 under the supervision of Claude Piguet. He is currently a postdoctoral fellow at the University of California, Berkeley (USA).

Inès Taarit obtained her Master degree in chemistry from the University Paris—Sorbonne in 2018, and she is working toward her doctoral degree in the group of Claude Piguet at the University of Geneva.

Homayoun Nozary obtained his Ph.D. degree in 2001 in the field of lanthanide-containing liquid crystals under the supervision of Claude Piguet at the University of Geneva. After postdoctoral work in the field of mass spectrometry, he moved to Canada in 2005 to work as R&D researcher in Photochimie St-Jean Inc. In 2007, he joined the Department of Inorganic Chemistry of the University of Geneva as a senior scientist and lecturer.

Alexandre Fürstenberg obtained his doctoral degree in the field of ultrafast spectroscopy with Prof. Eric Vauthey at the University of Geneva in 2007. After moving into single-molecule spectroscopy and imaging working with William E. Moerner at Stanford University, he is now a group leader at the University of Geneva jointly between the Department of Inorganic and Analytical Chemistry and Department of Physical Chemistry.

Claude Piguet earned a Ph.D. degree in 1989 in coordination chemistry (Alan F. Williams). After postdoctoral work in supramolecular chemistry (Jean-Marie Lehn) and lanthanide chemistry (Jean-Claude G. Bünzli), he was appointed as a full professor of inorganic chemistry at the University of Geneva (1999, successor to Christian K. Jørgensen).

ACKNOWLEDGMENTS

We acknowledge the Swiss National Science Foundation for long-term support, most recently via Grant 200020_178758. We express our deep appreciation for fruitful collaborations with Dr. Lilit Aboshyan-Sorgho, Dr. Gérald Bernardinelli, Dr. Céline Besnard, Prof. Jean-Claude Bünzli, Dr. Svetlana Eliseeva, Dr. Laure Guénée, Prof. Andreas Hauser, Prof. Stéphane Petoud, Dr. Yan Suffren, and Dr. Davood Zare who made these discoveries possible.

REFERENCES

(1) Suffren, Y.; Zare, D.; Eliseeva, S. V.; Guénée, L.; Nozary, H.; Lathion, T.; Aboshyan-Sorgho, L.; Petoud, S.; Hauser, A.; Piguet, C. Near-Infrared to Visible Light-Upconversion in Molecules: From Dream to Reality. *J. Phys. Chem. C* **2013**, *117*, 26957−26963.

(2) Suffren, Y.; Golesorkhi, B.; Zare, D.; Guénée, L.; Nozary, H.; Eliseeva, S. V.; Petoud, S.; Hauser, A.; Piguet, C. Taming Lanthanide-Centered Upconversion at the Molecular Level. *Inorg. Chem.* **2016**, *55*, 9964−9972.

(3) Golesorkhi, B.; Taarit, I.; Bolvin, H.; Nozary, H.; Jimenez, J. R.; Besnard, C.; Guenee, L.; Furstenberg, A.; Piguet, C. Molecular Light-Upconversion: We Have Had a Problem! When Excited State Absorption (ESA) Overcomes Energy Transfer Upconversion (ETU) in Cr(III)/Er(III) Complexes. *Dalton Trans.* **2021**, *50*, 7955−7968.

(4) Golesorkhi, B.; Naseri, S.; Guénée, L.; Taarit, I.; Alves, F.; Nozary, H.; Piguet, C. Ligand-Sensitized Near-Infrared to Visible Linear Light Upconversion in a Discrete Molecular Erbium Complex. *J. Am. Chem. Soc.* **2021**, *143*, 15326−15334.

(5) Van der Ende, B. M.; Aarts, L.; Meijerink, A. Lanthanide Ions as Spectral Converters for Solar Cells. *Phys. Chem. Chem. Phys.* **2009**, *11*, 11081−11095.

(6) Sabbatini, N.; Guardigli, M.; Manet, I. Antenna Effect in Encapsulation Complexes of Lanthanide Ions. *Handbook on the Physics and Chemistry of Rare Earths*; Gschneidner, K. A., Eyring, L., Eds.; Elsevier Science: Amsterdam, 1996; Vol. *23*, pp 69−120.

(7) Blau, W.; Dankesreiter, W.; Penzkofer, A. Saturable Absorption of Dyes Excited to the Long-Wavelength Region of the S0-S1 Absorption-Band. *Chem. Phys.* **1984**, *85*, 473−479.

(8) Auzel, F. Upconversion and Anti-Stokes Processes with f and d Ions in Solids. *Chem. Rev.* **2004**, *104*, 139−173.

(9) Aboshyan-Sorgho, L.; Nozary, H.; Aebischer, A.; Bünzli, J.-C. G.; Morgantini, P.-Y.; Kittilstved, K. R.; Hauser, A.; Eliseeva, S. V.; Petoud, S.; Piguet, C. Optimizing Millisecond Time Scale Near-Infrared Emission in Polynuclear Chrome(III)-Lanthanide(III) Complexes. *J. Am. Chem. Soc.* **2012**, *134*, 12675−12684.

(10) Prasad, P. N.; Williams, D. J. *Introduction to Nonlinear Optical effects in Molecules and Polymers*; John Wiley& Sons, New York, 1991.

(11) Pascal, S.; David, S.; Andraud, C.; Maury, O. Near-Infrared Dyes for Two-Photon Absorption in the Short-Wavelength Infrared:

Strategies Towards Optical Power Limiting. *Chem. Soc. Rev.* **2021**, *50*, 6613−6658.
(12) Scully, M. O.; Wodkiewicz, K.; Zubairy, M. S.; Bergou, J.; Lu, N.; Meyer ter Vehn, J. M. 2-Photon Correlated-Spontaneous-Emission Laser - Quantum Noise Quenching and Squeezing. *Phys. Rev. Lett.* **1988**, *60*, 1832−1835.
(13) Andraud, C.; Maury, O. Lanthanide Complexes for Nonlinear Optics: from Fundamental Aspects to Applications. *Eur. J. Inorg. Chem.* **2009**, *2009*, 4357−4371.
(14) Soulié, M.; Latzko, F.; Bourrier, E.; Placide, V.; Butler, S. J.; Pal, R.; Walton, J. W.; Baldeck, P. L.; Le Guennic, B.; Andraud, C.; Zwier, J. M.; Lamarque, L.; Parker, D.; Maury, O. Comparative Analysis of Conjugated Alkynyl Chromophore-Triazacyclononane Ligands for Sensitized Emission of Europium and Terbium. *Chem.—Eur. J.* **2014**, *20*, 8636−8646.
(15) Bloembergen, N. Solid State Infrared Quantum Counters. *Phys. Rev. Lett.* **1959**, *2*, 84−85.
(16) Porter, J. F. Fluorescence Excitation by Absorption of 2 Consecutive Photons. *Phys. Rev. Lett.* **1961**, *7*, 414−415.
(17) Pollnau, M.; Gamelin, D. R.; Lüthi, S. R.; Güdel, H. U.; Hehlen, M. P. Power Dependence of Upconversion Luminescence in Lanthanide and Transition-Metal-Ion Systems. *Phys. Rev. B* **2000**, *61*, 3337−3346.
(18) Golesorkhi, B.; Nozary, H.; Fürstenberg, A.; Piguet, C. Erbium Complexes as Pioneers for Implementing Linear Light-Upconversion in Molecules. *Mater. Horiz.* **2020**, *7*, 1279−1296.
(19) Bharmoria, P.; Bildirir, H.; Moth-Poulsen, K. Triplet-Triplet Annihilation Based Near Infrared to Visible Molecular Photon Upconversion. *Chem. Soc. Rev.* **2020**, *49*, 6529−6554.
(20) Khnayzer, R. S.; Blumhoff, J.; Harrington, J. A.; Haefele, A.; Deng, F.; Castellano, F. N. Upconversion-Powered Photoelectrochemistry. *Chem. Commun.* **2012**, *48*, 209−211.
(21) Brik, M. G.; Ma, C.-G. *Theoretical Spectroscopy of Transition Metal and Rare Earth Ions*; Jenny Stanford Publishing: Singapore, 2020.
(22) Gamelin, D. R.; Güdel, H. U. Design of Luminescent Inorganic Materials: New Photophysical Processes Studied by Optical Spectroscopy. *Acc. Chem. Res.* **2000**, *33*, 235−242.
(23) Chen, G.; Qiu, H.; Prasad, P. N.; Chen, X. Upconversion Nanoparticles: Design, Nanochemistry, and Applications in Theranostics. *Chem. Rev.* **2014**, *114*, 5161−5214.
(24) Baride, A.; May, P. S.; Berry, M. T. Cross-Relaxation from $Er^{3+}(^2H_{11/2}, {}^4S_{3/2})$ and $Er^{3+}(^2H_{9/2})$ in β-$NaYF_4$:Yb,Er and Implications for Modeling Upconversion Dynamics. *J. Phys. Chem. C* **2020**, *124*, 2193−2201.
(25) Browne, W. R.; O'Boyle, N. M.; McGarvey, J. J.; Vos, J. G. Elucidating Excited State Electronic Structure and Intercomponent Interactions in Multicomponent and Supramolecular Systems. *Chem. Soc. Rev.* **2005**, *34*, 641−663.
(26) Tanner, P. A.; Zhou, L.; Duan, C.; Wong, K.-L. Misconceptions in Electronic Energy Transfer: Bridging the Gap between Chemistry and Physics. *Chem. Soc. Rev.* **2018**, *47*, 5234−5265.
(27) Auzel, F. Compteur Quantique par Transfert d'Energie de Yb(III) à Tm(III) dans un Tungstate Mixte et dans un Verre Germanate. *C. R. Acad. Sc. Paris* **1966**, *B263*, 819−821.
(28) Inokuti, M.; Hirayama, F. Influence of Energy Transfer by the Exchange Mechanism on Donor Luminescence. *J. Chem. Phys.* **1965**, *43*, 1978−1989.
(29) Charbonnière, L. J. Bringing Upconversion down to the Molecular Scale. *Dalton Trans.* **2018**, *47*, 8566−8570.
(30) Nonat, A. M.; Charbonnière, L. J. Upconversion of Light with Molecular and Supramolecular Lanthanide Complexes. *Coord. Chem. Rev.* **2020**, *409*, 213192.
(31) Reinhard, C.; Güdel, H. U. High-Resolution Optical Spectroscopy of $Na_3[Ln(dpa)_3]\bullet 13H_2O$ with Ln = Er, Tm, Yb. *Inorg. Chem.* **2002**, *41*, 1048−1055.
(32) Xiao, X.; Haushalter, J. P.; Faris, G. W. Upconversion from Aqueous Phase Lanthanide Chelates. *Opt. Lett.* **2005**, *30*, 1674−1676.
(33) Blackburn, O. A.; Tropiano, M.; Sorensen, T. J.; Thom, J.; Beeby, A.; Bushby, L. M.; Parker, D.; Natrajan, L. S.; Faulkner, S. Luminescence and Upconversion from Thulium(III) Species in Solution. *Phys. Chem. Chem. Phys.* **2012**, *14*, 13378−13384.
(34) Sorensen, T. J.; Blackburn, O. A.; Tropiano, M.; Faulkner, S. Direct Two-Photon Excitation of Sm(III), Eu(III), Tb(III), Tb(DOTA), and Tb(DO3A) in Solution. *Chem. Phys. Lett.* **2012**, *541*, 16−20.
(35) Nonat, A.; Chan, C. F.; Liu, T.; Platas-Iglesias, C.; Liu, Z. Y.; Wong, W. T.; Wong, W. K.; Wong, K. L.; Charbonniere, L. J. Room Temperature Molecular Up Conversion in Solution. *Nat. Commun.* **2016**, *7*, 11978.
(36) Golesorkhi, B.; Guénée, L.; Nozary, H.; Fürstenberg, A.; Suffren, Y.; Eliseeva, S. V.; Petoud, S.; Hauser, A.; Piguet, C. Thermodynamic Programming of Erbium(III) Coordination Complexes for Dual Visible/Near-Infrared Luminescence. *Chem.—Eur. J.* **2018**, *24*, 13158−13169.
(37) Golesorkhi, B.; Nozary, H.; Guénée, L.; Fürstenberg, A.; Piguet, C. Room-Temperature Linear Light Upconversion in a Mononuclear Erbium Molecular Complex. *Angew. Chem., Int. Ed.* **2018**, *57*, 15172−15176.
(38) Golesorkhi, B.; Fürstenberg, A.; Nozary, H.; Piguet, C. Deciphering and Quantifying Linear Light Upconversion in Molecular Erbium Complexes. *Chem. Sci.* **2019**, *10*, 6876−6885.
(39) Sun, C.-Y.; Zheng, X.-J.; Chen, X.-B.; Jin, L.-P.; Li, L.-C. Assembly and Upconversion Luminescence of Lanthanide-Organic Frameworks with Mixed Acid Ligands. *Inorg. Chim. Acta* **2009**, *362*, 325−330.
(40) Balashova, T. V.; Pushkarev, A. P.; Yablonskiy, A. N.; Andreev, B. A.; Grishin, I. D.; Rumyantcev, R. V.; Fukin, G. K.; Bochkarev, M. N. Organic Er-Yb Complexes as Potential Upconversion Materials. *J. Luminesc.* **2017**, *192*, 208−210.
(41) Li, M.; Gul, S.; Tian, D.; Zhou, E.; Wang, Y.; Han, Y.-F.; Yin, L.; Huang, L. Erbium-Based Metal-Organic Frameworks with Tunable Upconversion Emissions. *Dalton Trans.* **2018**, *47*, 12868−12872.
(42) Hyppänen, I.; Lahtinen, S.; Ääritalo, T.; Mäkelä, J.; Kankare, J.; Soukka, T. Photon Upconversion in a Molecular Lanthanide Complex in Anhydrous Solution at Room Temperature. *ACS Photonics* **2014**, *1*, 394−397.
(43) Monteiro, J.; Hiti, E. A.; Hardy, E. E.; Wilkinson, G. R.; Gorden, J. D.; Gorden, A. E. V.; de Bettencourt-Dias, A. New Up-conversion Luminescence in Molecular Cyano-Substituted Naphthylsalophen Lanthanide(III) Complexes. *Chem. Commun.* **2021**, *57*, 2551−2554.
(44) Wang, J.; Jiang, Y.; Liu, J. Y.; Xu, H. B.; Zhang, Y. X.; Peng, X.; Kurmoo, M.; Ng, S. W.; Zeng, M. Discrete Heteropolynuclear Yb/Er Assemblies: Switching on Molecular Upconversion under Mild Conditions. *Angew. Chem., Int. Ed.* **2021**, *60*, 22368−22375.
(45) Aboshyan-Sorgho, L.; Besnard, C.; Pattison, P.; Kittilstved, K. R.; Aebischer, A.; Bünzli, J.-C. G.; Hauser, A.; Piguet, C. Near-Infrared to Visible Light Upconversion in a Molecular Trinuclear d-f-d Complex. *Angew. Chem., Int. Ed.* **2011**, *50*, 4108−4112.
(46) Zare, D.; Suffren, Y.; Guénée, L.; Eliseeva, S. V.; Nozary, H.; Aboshyan-Sorgho, L.; Petoud, S.; Hauser, A.; Piguet, C. Smaller than a Nanoparticle with the Design of Discrete Polynuclear Molecular Complexes Displaying Near-Infrared to Visible Upconversion. *Dalton Trans.* **2015**, *44*, 2529−2540.
(47) Aboshyan-Sorgho, L.; Cantuel, M.; Petoud, S.; Hauser, A.; Piguet, C. Optical Sensitization and Upconversion in Discrete Polynuclear Chromium-Lanthanide Complexes. *Coord. Chem. Rev.* **2012**, *256*, 1644−1663.
(48) Suzuki, H.; Nishida, Y.; Hoshino, S. Ligand-sensitized and Upconversion Photoluminescence in Vacuum-deposited Thin Films of an Infrared Electroluminescent Organic Erbium Complex. *Mol. Cryst. Liq. Cryst.* **2003**, *406*, 27−37.
(49) Stavola, M.; Dexter, D. L. Energy-Transfer and 2-Center Optical-Transitions Involving Rare-Earth and OH^- Impurities in Condensed Matter. *Phys. Rev. B* **1979**, *20*, 1867−1885.
(50) Souri, N.; Tian, P.; Lecointre, A.; Lemaire, Z.; Chafaa, S.; Strub, J.-M.; Cianferani, S.; Elhabiri, M.; Platas-Iglesias, C.; Charbonnière, L. J. Step-by-step Assembly of Polynuclear Lanthanide Complexes with a

https://doi.org/10.1021/acs.accounts.1c00685
Acc. Chem. Res. 2022, 55, 442−456

Phosphonated Bipyridine Ligand. *Inorg. Chem.* **2016**, *55*, 12962−12974.
(51) Souri, N.; Tian, P.; Platas-Iglesias, C.; Wong, K.-L.; Nonat, A.; Charbonnière, L. J. Upconverted Photosensitization of Tb Visible Emission by NIR Yb Excitation in Discrete Supramolecular Heteropolynuclear Complexes. *J. Am. Chem. Soc.* **2017**, *139*, 1456−1459.
(52) Salaam, J.; Tabti, L.; Bahamyirou, S.; Lecointre, A.; Hernandez Alba, O.; Jeannin, O.; Camerel, F.; Cianférani, S.; Bentouhami, E.; Nonat, A.; Charbonnière, L. J. Formation of Mono- and Polynuclear Luminescent Lanthanide Complexes Based on the Coordination of Preorganized Phosphonated Pyridines. *Inorg. Chem.* **2018**, *57*, 6095−6106.
(53) Charpentier, C.; Salaam, J.; Lecointre, A.; Jeannin, O.; Nonat, A.; Charbonnière, L. J. Phosphonated Podand Type Ligand for the Complexation of Lanthanide Cations. *Eur. J. Inorg. Chem.* **2019**, *2019*, 2168−2174.
(54) Nonat, A.; Bahamyirou, S.; Lecointre, A.; Przybilla, F.; Mély, Y.; Platas-Iglesias, C.; Camerel, F.; Jeannin, O.; Charbonnière, L. J. Molecular Upconversion in Water in Heteropolynuclear Supramolecular Tb/Yb Assemblies. *J. Am. Chem. Soc.* **2019**, *141*, 1568−1576.
(55) Petit, S.; Baril-Robert, F.; Pilet, G.; Reber, C.; Luneau, D. Luminescence Spectroscopy of Europium(III) and Terbium(III) Penta-, Octa- and Nonanuclear Clusters with Beta-Diketonate Ligands. *Dalton Trans.* **2009**, 6809−6815.
(56) Knighton, R. C.; Soro, L. K.; Lecointre, A.; Pilet, G.; Fateeva, A.; Pontille, L.; Frances-Soriano, L.; Hildebrandt, N.; Charbonniere, L. J. Upconversion in Molecular Hetero-nonanuclear Lanthanide Complexes in Solution. *Chem. Commun.* **2021**, *57*, 53−56.
(57) Hernandez, I.; Pathumakanthar, N.; Wyatt, P. B.; Gillin, W. P. Cooperative Infrared to Visible Up Conversion in Tb^{3+}, Eu^{3+} and Yb^{3+} Containing Polymers. *Adv. Mater.* **2010**, *22*, 5356−5360.
(58) Ye, H.; Bogdanov, V.; Liu, S.; Vajandar, S.; Osipowicz, T.; Hernandez, I.; Xiong, Q. Bright Photon Upconversion on Composite Organic Lanthanide Molecules Through Localized Thermal Radiation. *J. Phys. Chem. Lett.* **2017**, *8*, 5695−5699.
(59) Kalmbach, J.; Wang, C.; You, Y.; Forster, C.; Schubert, H.; Heinze, K.; Resch-Genger, U.; Seitz, M. Near-IR to Near-IR Upconversion Luminescence in Molecular Chromium Ytterbium Salts. *Angew. Chem., Int. Ed.* **2020**, *59*, 18804−18808.
(60) Dasari, S.; Singh, S.; Kumar, P.; Sivakumar, S.; Patra, A. K. Near-Infrared Excited Cooperative Upconversion in Luminescent Ytterbium-(III) Bioprobes as Light-Responsive Theranostic Agents. *Eur. J. Med. Chem.* **2019**, *163*, 546−559.
(61) Richards, B. S.; Hudry, D.; Busko, D.; Turshatov, A.; Howard, I. A. Photon Upconversion for Photovoltaics and Photocatalysis: A Critical Review. *Chem. Rev.* **2021**, *121*, 9165−9195.
(62) Sveshnikova, E. B.; Ermolaev, V. L. Inductive-Resonant Theory of Nonradiative Transitions in Lanthanide and Transition Metal Ions. *Opt. Spectrosc.* **2011**, *111*, 34−50.
(63) Lemonnier, J.-F.; Guénée, L.; Beuchat, C.; Wesolowski, T. A.; Mukherjee, P.; Waldeck, D. H.; Gogick, K. A.; Petoud, S.; Piguet, C. Optimizing Sensitization Processes in Dinuclear Luminescent Lanthanide Oligomers: Selection of Rigid Aromatic Spacers. *J. Am. Chem. Soc.* **2011**, *133*, 16219−16234.
(64) Chen, F.-F.; Chen, Z.-Q.; Bian, Z.-Q.; Huang, C.-H. Sensitized Luminescence from Lanthanides in d-f Bimetallic Complexes. *Coord. Chem. Rev.* **2010**, *254*, 991−1010.
(65) Xu, L.-J.; Xu, G.-T.; Chen, Z.-N. Recent Advances in Lanthanide Luminescence with Metal-Organic Chromophores as Sensitizers. *Coord. Chem. Rev.* **2014**, *273*−*274*, 47−62.
(66) Faulkner, S.; Natrajan, L. S.; Perry, W. S.; Sykes, D. Sensitised Luminescence in Lanthanide Containing Arrays and d-f Hybrids. *Dalton Trans.* **2009**, 3890−3899.
(67) Debroye, E.; Parac-Vogt, T. N. Towards Polymetallic Lanthanide Complexes as Dual Contrast Agents for Magnetic Resonance and Optical Imaging. *Chem. Soc. Rev.* **2014**, *43*, 8178−8192.
(68) Sorensen, T. J.; Faulkner, S. Multimetallic Lanthanide Complexes: Using Kinetic Control to Define Complex Multimetallic Arrays. *Acc. Chem. Res.* **2018**, *51*, 2493−2501.
(69) Aguila, D.; Roubeau, O.; Aromi, G. Designed Polynuclear Lanthanide Complexes for Quantum Information Processing. *Dalton Trans.* **2021**, *50*, 12045−12057.
(70) Knighton, R. C.; Soro, L. K.; Frances-Soriano, L.; Rodriguez-Rodriguez, A.; Pilet, G.; Lenertz, M.; Platas-Iglesias, C.; Hildebrandt, N.; Charbonniere, L. J. Cooperative Luminescence and Cooperative Sensitisation Upconversion of Lanthanide Complexes in Solution. *Angew. Chem., Int. Ed.* **2021**, *61*, e202113114.

https://doi.org/10.1021/acs.accounts.1c00685
Acc. Chem. Res. 2022, 55, 442−456